

# Environmental Science Advances

Volume 2  
Number 2  
February 2023  
Pages 143–348

rsc.li/esadvances



ISSN 2754-7000

## TUTORIAL REVIEW

Baljit Singh *et al.*  
Review of analytical techniques for arsenic detection  
and determination in drinking water



Cite this: *Environ. Sci.: Adv.*, 2023, 2, 171

## Review of analytical techniques for arsenic detection and determination in drinking water

Abhijnan Bhat,<sup>1</sup> Tony O Hara,<sup>2</sup> Furong Tian<sup>3</sup> and Baljit Singh<sup>4</sup>\*

Arsenic occurs in the natural environment in four oxidation states: As(v), As(III), As(0) and As(-III). The behavior of arsenic species changes depending on the biotic or abiotic conditions in water. In groundwater, arsenic is predominantly present as As(III) and As(v), with a minor amount of methyl and dimethyl arsenic compounds being reported. Global intake of As(III) and As(v) via drinking water and food has dramatically increased in recent years. The commonly used term inorganic arsenic includes both As(III) and As(v) species and constitutes the highest toxicological risk associated with arsenic in water compared to the organic arsenic species. Inorganic arsenic is a confirmed carcinogen and the World Health Organization (WHO) has published a guideline value for arsenic in their 'Guidelines for drinking-water quality' and is on the WHO list of 10 chemicals of major public health concern. Presently, approximately, 230 million people worldwide are affected by arsenic toxicity. Chronic arsenic toxicity affects multiple physiological systems and can cause serious health issues (e.g. arsenicosis, cancer etc.) leading to death. To combat arsenic pollution, the WHO and United States Environmental Protection Agency (US-EPA) have set concentration limits for arsenic in drinking water. The WHO, US-EPA and European Union (EU) have set the maximum limit of arsenic in drinking water at 10 ppb. To meet the required limit, it is essential that rapid, reliable, sensitive and cost-effective analytical detection systems be developed and put into use. Different determination methods of inorganic arsenic have been developed over the last 5–6 decades. This review provides an overview of around 170 research articles and relevant literature, mainly regarding the existing methods for analysis of As(III) and As(v) in water. Chromatographic, spectroscopic, colorimetric, biological (whole cell biosensors (WCB) and aptasensors), electroanalytical and coupled techniques are discussed. For those who are at the early stage of their research career in this field, the basic introduction and necessary concepts for various techniques is discussed followed by an evaluation of their performance towards arsenic determination. Current challenges as well as potential avenues for future research, including the demands for enhanced analytical performance, rapid analysis and on-site technologies for remote water analysis and environmental applications are discussed. We believe that this review will be beneficial, a source of information, and enhance awareness and appreciation of the role of these advanced analytical techniques in informing and protecting our environment and water resources, globally.

Received 8th September 2022  
Accepted 4th November 2022

DOI: 10.1039/d2va00218c

rsc.li/esadvances

### Environmental significance

Global intake of arsenic via drinking water is a major environmental concern: As(III)/As(v) species constitutes the highest toxicological-risk. To combat arsenic pollution and associated toxicity, WHO and EPA have regulations, guidelines and introduced directives for arsenic concentration limits in drinking water. The existing laboratory-based methods are suitable for arsenic analysis but are time-consuming, expensive and require skilled analysts and extensive sample preparation. Rapid, cost-effective and reliable portable techniques and on-site sensor-based methods are the emerging needs. This review provides an overview of various analytical techniques for arsenic detection and determination in water, and will enhance awareness of their role in informing and protecting our environment and water resources, globally.

<sup>1</sup>MiCRA Biodiagnostics Technology Gateway, Technological University Dublin (TU Dublin), Dublin 24, D24 FKT9, Ireland. E-mail: Baljit.Singh@tudublin.ie; Tel: +353 1 220 7863

<sup>2</sup>Centre of Applied Science for Health, Technological University Dublin (TU Dublin), Dublin 24, D24 FKT9, Ireland

<sup>3</sup>School of Food Science & Environmental Health, Technological University Dublin (TU Dublin), Grangegorman, Dublin 7, D07 H6K8, Ireland

<sup>4</sup>Pesticide Registration Division, Department of Agriculture, Food and the Marine, Backweston Laboratory Campus, Celbridge, County Kildare W23 VW2C, Ireland

## 1. Introduction

Water covers more than 70% of our planet's surface. Because life on Earth began in water, it is not surprising that all living organisms on our blue planet require water. Water is in fact the most valuable environmental natural resource, vital to global need, a transport corridor and a climate regulator. Global intake



of arsenic *via* drinking water and food has dramatically increased, recently. Arsenic contamination in groundwater can occur naturally, geologically or through industrial effluents, agricultural (*e.g.* insecticides) usage, municipal sewage, and household waste (Fig. 1).<sup>1</sup> Depending on the physical, chemical and biogeochemical processes and condition of the environment, various arsenic species can be present in water. Water

soluble arsenic species existing in natural water are inorganic arsenic and organic arsenic and their distribution is a function of pH.<sup>2</sup>

Arsenic exists in four oxidation states in nature: As(v), As(III), As(0), and As(-III) (Fig. 2). The behavior of arsenic species changes depending on the biotic or abiotic conditions in water. In groundwater, arsenic is predominantly present as As(III) and



*Abhijnan Bhat has completed his M.Sc. (Chemistry, 2021) from Central University of Punjab (India). Presently, he is working as a PhD research scholar at Technological University Dublin (TU Dublin, Ireland) under the supervision of Dr Baljit Singh and Dr Furong Tian. Previously, he completed his B.Sc (Honours, Chemistry, 2019) at Ramakrishna Mission Vidyamandira, Belur Math*

*(India). His PhD research involves the analytical and electroanalytical techniques for arsenic detection and determination in drinking water. Research interests: Analytical techniques, nanomaterials, electrochemical sensors, water & environmental contaminants, arsenic research.*



*Dr Furong Tian obtained her PhD at Maxplanck Institute for metal research and postdoc in National institute for material science in Japan. She was Marie Curie Post doc in FOCAS research Institute (TU Dublin). Research interests: Her research interest focuses on smart instrument for disease diagnosis and treatment based on nanomaterials and biosensors, point-of-care lateral strip, smart nanoscale drug delivery system.*



*Dr Tony O Hara works as an Environmental Chemist at the Department of Agriculture, Food & Marine, Ireland. He was previously employed at the State Laboratory Ireland. Prior to this, Tony worked as a Postdoctoral Researcher at the School of Chemical Sciences, Dublin City University where he aided in the development of a prototype electrolyser for green hydrogen generation. Tony completed his*

*PhD in 2016 at the Technological University Dublin. His PhD research involved the development of a whole cell electrochemical biosensor for environmental toxicant screening applications. Research interests: Development of electrochemical sensors/biosensors for environmental sensing applications.*



*Dr Baljit Singh is a Principal Investigator and Senior-Business-Development-Professional (TU Dublin), contributing to applied research/teaching, business-development/management, and commercialization activities. Dr Singh contributed immensely to the establishment of Enterprise-Ireland Technology Gateway 'MiCRA Biodiagnostics' and worked with a range of start-ups,*

*SMEs, and multinational companies. He delivered several collaborative industry-research projects and is a key contributor to the innovation-technologies developed at MiCRA Biodiagnostics. He received M.Tech (Advanced-Chemical-Analysis, IIT-Roorkee, India), PhD in Electroanalytical Chemistry/Sensors-Nanomaterials (TU Dublin) followed by Postdoctoral, Senior-Postdoctoral-Research-Fellow and Business-Development positions. Dr Singh worked as a Lecturer and Associate Lecturer (Chemistry, TU Dublin) and previously as Lecturer (Chemistry, D.A.V. College, Pehowa, India). Dr Singh is a Guest Editor: Biosensors & Chemosensors (MDPI), and reviewed number of articles for RSC, ACS, Elsevier journals. Research interests: Electrochemical sensors/biosensors development, point-of-care devices, nanomaterials, design-engineering of electrode-detection & microfluidic-reagent systems.*



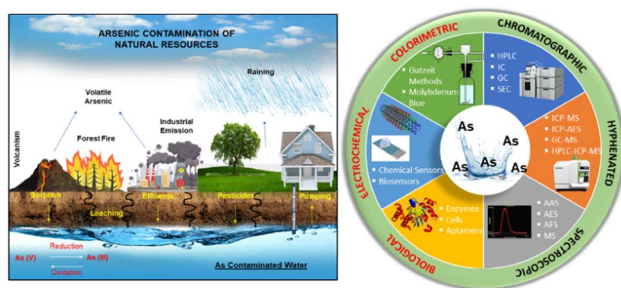


Fig. 1 Schematic representation of human exposure to arsenic and arsenic cycle (left). Various analytical methods for arsenic determination (right).

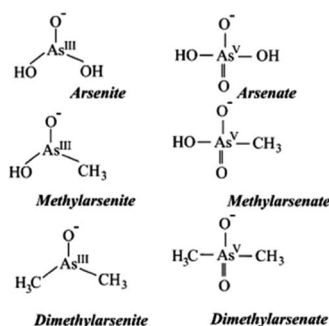


Fig. 2 Different arsenic species found in water<sup>3</sup> (reprinted from ref. 3; Copyright (2004), with permission from Elsevier).

As(v), with a minor amount of methyl and dimethyl arsenic compounds being reported.<sup>3</sup> The term inorganic arsenic includes both As(III) and As(v) species and constitutes the highest toxicological risk associated with arsenic in water in contrast to the organic arsenic species. The WHO has published a guideline value for arsenic in its Guidelines for drinking-water quality and arsenic is on their list of 10 chemicals of major public health concern.<sup>4</sup> Presently, more than 230 million people worldwide are affected by arsenic toxicity.<sup>5</sup> Acute arsenic toxicity has been reported to cause acute paralytic syndrome (APS) and acute gastrointestinal syndrome (AGS).<sup>6</sup> Chronic arsenic toxicity affects multiple physiological systems and can cause serious health issues *e.g.* black-foot illnesses, arsenicosis, cancer, *etc.* Numerous epidemiological studies have examined the risk of cancers associated with the arsenic absorption through drinking water. There is significant evidence that greater arsenic levels in drinking water are linked to cancer growth including the skin, bladder, and lungs related cancers. The International Agency for Research on Cancer (IARC) classified arsenic and inorganic arsenic as “carcinogenic to humans” (group 1).<sup>7</sup>

To combat arsenic pollution and associated toxicity, the WHO, US-EPA and EU have guidelines, regulations and directives that set concentration limits for arsenic in drinking, surface and ground water. Also, due to the toxic potential of inorganic As, the European Food Safety Authority (EFSA) recommends minimizing its intake and the European

Commission has set the maximum levels.<sup>7</sup> WHO, EU and US-EPA maximum limit for arsenic in drinking water is 10 ppb.<sup>8,9</sup> To meet this value, it is essential that rapid, sensitive, cost-effective and reliable analytical detection systems be developed and put into use.

Determination of arsenic species is of crucial importance to define the limits and safety of drinking water as well as in selection of arsenic removal technology for groundwater applications. The importance of arsenic determination is well-recognised and emphasised by the extensive studies carried out in this space *e.g.* “Arsenic round the world: a review”.<sup>7,10</sup> A plethora of detection methods have been developed and reported and some are capable of detecting arsenic below the WHO guideline value of 10 ppb (Fig. 3).<sup>11,12</sup> The most selective and sensitive methods for determination of total arsenic and its species in water are coupled techniques including chromatography, optical methods and mass spectrometry.<sup>2,11,12</sup> Coupled techniques are where combined methods *e.g.* chromatographic and spectroscopic are used to determine arsenic levels. Colorimetric, biological, electrochemical techniques have also been reported for the arsenic determination.<sup>13–17</sup> Most of the existing methods are suitable for laboratory conditions only and analysis is time consuming and can lead to a large capital cost for multi-sample analysis hence not suitable for routine monitoring of large numbers of samples. Therefore, rapid, cost-effective, reliable and portable techniques such as on-site sensor-based methods are crucial. In this regard, the use of electrochemical methodologies has recently come to the forefront of research as a possible means of fulfilling these requirements.

The purpose of this review is to provide an overview of the analytical techniques (chromatographic, spectroscopic, colorimetric, biological, electroanalytical and coupled techniques) for arsenic determination in drinking water and the authors have mostly covered the literature over the past decade (2010 onwards). Some older publications are referenced to support the key concepts and wherever necessary. A brief introduction to various analytical techniques followed by an evaluation of their capabilities and performance for arsenic determination are discussed. Associated challenges as well as potential avenues for future research, including the demand for rapid analysis and on-site technologies for remote water analysis and environmental applications are discussed. We hope that this review

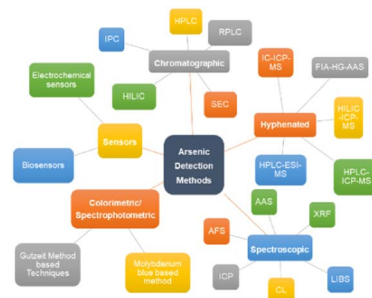


Fig. 3 Different methods of arsenic detection and determination.



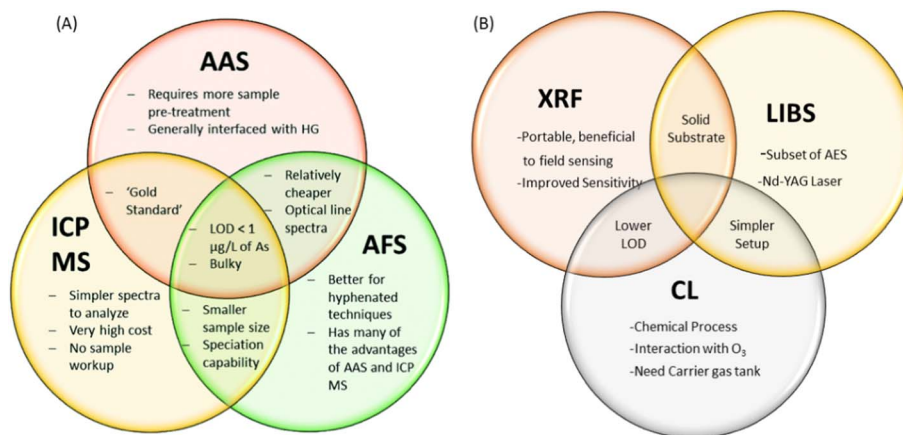


Fig. 4 (A) Illustration of spectroscopic methods: AAS, ICP MS and AFS<sup>11</sup> (reproduced from ref. 11 with permission from the Royal Society of Chemistry, Copyright [2015]), (B) XRF, LIBS and CL for detection of arsenic.

will be of benefit to those working in the area of water and environmental analysis in particular to the postgraduate students, early-stage researchers and scientists. Overall, this review will enhance awareness and appreciation of the role that these advanced analytical techniques play in informing and protecting our environment and water resources, globally.

## 2. Analytical methods & techniques for arsenic determination

### 2.1. Spectroscopic methods

The general performance attributes of atomic absorption spectroscopy (AAS), inductively coupled plasma mass spectrometry (ICP-MS) and atomic fluorescence spectroscopy (AFS) are illustrated for trace arsenic detection in water samples in Fig. 4. All of these listed techniques can accurately perform high throughput sample analyses with good reproducibility. Most accepted laboratory methods have a limit of detection (LOD) for arsenic on the order of 1 part per billion (ppb). The spectroscopic analysis of solid matrices is frequently used in environmental chemistry. Two solid-state analysis techniques that have been investigated for arsenic detection are laser induced breakdown spectroscopy (LIBS) and X-ray fluorescence (XRF). Another spectroscopic technique, chemiluminescence (CL),

detects arsenic in its gaseous state.<sup>11</sup> The relevant literature on the spectroscopic techniques is summarised in the Table 1.

**2.1.1. Atomic absorption spectroscopy.** AAS with vapour generation assembly (AAS-VGA) is well known technique for the trace analysis of arsenic. However, total arsenic analysis [As(III) + As(V)] is critical, and proper analysis needs conversion of As(V) to As(III). As(III) is converted to AsH<sub>3</sub> vapors, and then free As atoms, which are responsible for the AAS absorption signal. To do this, the AAS-attached vapor generation assembly has an acid channel filled with 10 M HCl and a reduction channel filled with sodium borohydride.<sup>18</sup> Graphite furnace atomic absorption spectrometry (GFAAS) also has the potential to detect arsenic but the LOD is generally too high except for methods using a pre-concentration or separation step. Michon *et al.* tried to optimise the conditions to lower down the LOD.<sup>19</sup> The use of a high-intensity boosted discharge hollow-cathode lamp decreased the baseline noise level and therefore allowed a lower LOD of 0.26 ppb for a sample volume of 16 µL corresponding to 4.2 pg As.<sup>19</sup>

**2.1.2. Atomic fluorescence spectroscopy.** AFS represents a suitable alternative to other atomic spectrometers commonly employed in speciation studies such as AAS and ICP-MS.<sup>20</sup> AFS has been described to be superior to AAS and similar to ICP-MS regarding sensitivity and linear calibration range, with further advantages (simplicity, lower acquisition and running costs) for

Table 1 Performance comparison of spectroscopic techniques for trace arsenic detection in water samples

Techniques	LOD (ppb)	Sample size (µL)	Time (min s <sup>-1</sup> )	Skills requirement	Ref
AAS	0.0009–1	>1000	~30 min	Easy to use for a trained technician	11, 18 and 31
ICP-MS	0.0003–1	2–200	~30 s	Difficult initial method development even for a trained technician	11, 24, 32 and 33
AFS	0.0003–10	20–200	~10 min	Easy to use for a trained technician	11, 23 and 33
XRF	0.7	NA	~20–22 min	Easy to handle for a trained technician	28, 29 and 34
LIBS	83	NA	NA	Easy to handle for a trained technician	26
CL	0.4	NA	~1 min	Relatively easy to handle	30 and 35



arsenic speciation.<sup>21,22</sup> AFS provides interesting analytical features, such as low LODs and wide linear calibration range (from ppb to ppm).<sup>23</sup>

**2.1.3. Inductively coupled plasma mass spectrometry (ICP-MS).** Determination of arsenic in drinking water requires a method where low levels of detection can be obtained. In the last decade, ICP-MS has become a method of choice in analysis of water samples of different origin. Double focusing sector field ICP-MS enables direct determination of elements of interest with no pre-concentration or isolation required. Next to the ability for multielement analysis, double focusing ICP-MS also offers high sensitivity over a wide linear range and low LODs.<sup>24</sup> For the detection of multiple arsenic species, ICP-MS is the most commonly used technique because of its high sensitivity selectivity, and wide dynamic range. To minimise or reduce isobaric interferences (equal mass isotopes of different elements present in the same sample) in the detection of arsenic at a mass-to-charge ratio of 75, various approaches have been developed. A collision/reaction cell can be used to reduce interfering ions in polyatomic interferences by adding collision gas (*e.g.*, helium), reaction gas (*e.g.*, oxygen, hydrogen, CH<sub>3</sub>F), or a mixture of two gases into the ICP-MS. When compared to standard single quadrupole ICP-MS, the use of ICP with triple quadrupole tandem mass spectrometry (ICP-QQQ) helps to remove isobaric interferences, reduce background noise, and improve selectivity.<sup>25</sup>

**2.1.4. Laser induced breakdown spectroscopy (LIBS).** LIBS is an atomic emission spectroscopy (AES) subset that employs energy from a laser pulse as the excitation source. Although there is literature on the use of LIBS for the analysis of solid, liquid, and gas state samples, the examination of solids is the most common. LIBS analysis of water samples, on the other hand, can be performed using a wood substrate.<sup>11</sup> The main advantage of LIBS is that the entire setup is quite simple, consisting of only a neodymium-doped yttrium aluminum garnet (Nd:YAG) laser, a high sensitivity spectrometer, and a computer for data acquisition. LIBS has been used to detect arsenic in solution at concentrations levels around 83 ppb.<sup>26</sup> This sensitivity has been achieved through concentration enhancement *via* boiling, followed by sample adsorption onto a zinc oxide substrate. However, miniaturised LIBS systems ( $\mu$ LIBS) have been developed for the elemental analyses of sodium and lead, which achieve similar sensitivities while analysing liquid samples directly.<sup>26</sup>

**2.1.5. X-ray fluorescence (XRF).** XRF has been used to analyze arsenic in water samples by pre-concentrating arsenic on solid substrates such as tape and alumina. The latter method, which involves pre-concentrating arsenic onto alumina particles and then centrifuging pellets for solid-state analysis, has a LOD of 0.7 ppb of arsenic in solution. It is possible to concentrate very high levels of arsenic into very small areas using microfluidics; this will likely improve sensitivity and eliminate the need for centrifugation. Some XRF detectors are already portable, which is an added benefit to field sensing.<sup>27–29</sup>

**2.1.6. Chemiluminescence (CL).** The creation of light as a result of a chemical process is known as chemiluminescence. For more than 30 years, the CL produced by the interaction of

arsenic and ozone (O<sub>3</sub>) has been known. Furthermore, the CL spectra of arsine gas and ozone are different. During CL analysis, arsenic is transformed to arsine gas *via* hydride generation, and then the arsine gas is delivered to an ozone chamber *via* a carrier gas flow for further reaction. This approach can detect arsenic levels on the order of 1 ppb. However, due to the need for a carrier gas tank, it is not very practical in the field.<sup>30</sup>

## 2.2. Chromatographic methods & hyphenated techniques

The different chromatographic techniques for arsenic detection and determination are shown in Fig. 5.

**2.2.1. Ion chromatography (IC) or ion-exchange chromatography (IEX).** IEX separates ions and polar molecules based on their affinity to the ion exchanger. IEX is often used to separate biological molecules such as large proteins, amino acids and small nucleotides. The charge carried by the target molecule can be easily controlled by using a buffer of a particular pH. This technique makes it possible to separate comparable sorts of molecules that would be challenging to separate by other techniques. The two types of IEX are (i) anion-exchange and (ii) cation-exchange. When the molecule of interest is positively charged, cation-exchange chromatography is used. The molecule is positively charged because the pH for chromatography is less than the isoelectric point (pI).<sup>36</sup> In this type of chromatography, the stationary phase is negatively charged and positively charged molecules are loaded to be attracted to it.<sup>37</sup> Anion-exchange chromatography is when the stationary phase is positively charged and negatively charged molecules (meaning that pH for chromatography is greater than the pI) are loaded to be attracted to it. One of the primary advantages for the use of IEX is only one interaction is involved during the separation as opposed to other separation techniques; therefore, IEX may have higher matrix tolerance. The regularity of elution patterns is another advantage of ion exchange (based on the presence of the ionizable group). Cations, for example, will elute out last in cation exchange chromatography. Meanwhile, the negatively charged molecules will be the first to elute.



Fig. 5 Different chromatographic techniques for arsenic detection.



However, there are also disadvantages involved when performing IEX, such as constant evolution with the technique which leads to the inconsistency from column to column.<sup>38</sup> One significant disadvantage of this purification approach is that it is only applicable to ionizable groups.<sup>36</sup>

**2.2.1.1. Anion exchange chromatography.** Anion exchange chromatography, in particular, employs a positively charged ion exchange resin with a preference for molecules with net negative surface charges. Anion exchange chromatography is used both for preparative and analytical purposes for various applications and can separate a large range of molecules but here we are discussing it for arsenic detection perspective. Under neutral pH, inorganic arsenic acid As(v), mono-methylarsonic acid (MMA), and dimethylarsinic acid (DMA) are deprotonated to form anionic species on the basis of the physicochemical properties ( $pK_a$  values) of these compounds, whereas inorganic arsenous acid As(III) exists as a neutral species. Anion exchange chromatography is a viable option for the separation of these common arsenic species due to differences in their anionic nature. As(v) is the slowest eluting compound because it has a strong negative charge in most mobile phases due to its low  $pK_{a_1}$  (2.19) and  $pK_{a_2}$  (6.98). As(III) has very little retention because it typically exists as a neutral compound due to its high  $pK_a$  values ( $pK_{a_1} = 9.23$ ,  $pK_{a_2} = 12.13$ ,  $pK_{a_3} = 13.4$ ). Anion exchange chromatography has been used in the analysis of many As compounds, including As(III), As(v), MMA, DMA, arsenobetaine (AsB), arsenocholine (AsC), oxo-arsenosugars (oxoAsS), thio-arsenosugars (thioAsS), and phenylarsenicals. The most commonly used column for arsenic speciation analysis is a strong anion exchange column, e.g., PRP-X100.<sup>12</sup>

**2.2.1.2. Cation exchange chromatography.** Just as anion exchange chromatography is used for analysis of anionic arsenic species, cation exchange chromatography is commonly used for speciation analysis of positively charged As compounds, such as AsB, AsC, trimethylarsine oxide (TMAO), and tetramethylarsonium ion (TMA). Cation exchange chromatography works in a similar manner to anion exchange except that the stationary phase is negatively charged so as to interact with cationic analytes. The retention of arsenicals is directly related to the strength of their cationic charge: stronger positively-charged analytes have greater retention. Wolle *et al.* used a strong cation exchange (PRP-X200) column to separate As(III), MMA, As(v), DMA, AsB, and TMAO, with AsC and TMA co-eluting, in 15 minute.<sup>39</sup> Chen *et al.* used cation exchange chromatography to confirm the presence of TMAO when performing arsenic speciation in rice samples.<sup>40</sup>

**2.2.2. Ion pair chromatography (IPC).** IPC is a form of ion chromatography used to separate hydrophilic or charged analytes on columns employing reversed phase or “neutral” stationary phases that do not carry charges. IPC is used for the separation of polar organic acids, bases and zwitterions as well as inorganic ions. IPC, which can separate both ionic and neutral species, has been frequently utilised for arsenic speciation analysis. IPC uses a standard reversed-phase column (C18) with ion pair reagents in the mobile phase. The charged group of the ion pair reagent interacts with the analyte, whereas the hydrophobic area interacts with the stationary phase.

Typically, tetraalkylammonium, tetra-butylammonium and tetraethylammonium are commonly used as the ion pair reagents for the speciation of anionic and neutral arsenic species. Alkyl sulfonates, such as hexane sulfonic acid and 1-pentane sulfonic acid, are commonly used in ion pair separation of cationic and neutral arsenic species. Methanol and acetonitrile are the two most often utilised organic modifiers. They are typically added to the mobile phase to shorten retention times and change selectivity. The neutral arsenic species can interact directly with the conventional stationary phase but the charged arsenic species must go *via* the ion pair reagents and the hydrophobic stationary phase in order to engage with it. Morita *et al.* devised a mixed ion pair method that separated As(v), As(III), MMA, DMA, AsB, TMAO, TMA, and AsC in less than 12 minutes utilising a combination of sodium butanesulfonate and tetramethylammonium hydroxide as the ion pairing reagents.<sup>41</sup> Nan *et al.* separated As(v), As(III), DMA, AsB, TMAO, TMA, and three new As species in under 15 minutes using a similar approach. The authors identified one of the unknown peaks as an arsenosugar (2,3-dihydroxypropyl-5-deoxy-5(dimethylarsenoso)furanoside) using ESI-MS.<sup>42</sup> Shi *et al.* used a Zorbax SB-Aq column with a mobile phase consisting of 20 mM citric acid and 5 mM sodium hexanesulfonate adjusted to a pH of 4.3 to achieve separation of As(III), As(v), MMA, and DMA in under 4 min.<sup>43</sup>

**2.2.3. Reversed-phase-liquid chromatography (RP-LC).** This is an incredibly powerful mode of separation that is applicable to a wide variety of applications, ranging from the separation of small organic acids to 150 kDa proteins. Reversed-phase separations have limitations, however, with one of the most practically significant ones being low retention for compounds that are highly water soluble (hydrophilic). RP-LC is particularly useful in the analysis of arsenolipids, which include arsenic-containing hydrocarbons, fatty acids, phospholipids, phosphatidylcholines, fatty alcohols, and phosphatidylethanolamines.<sup>44,45</sup> Typical C18 or C8 columns allow arsenolipids to be separated based on the number of carbons, number of double bonds, and other functional groups. For the measurement and identification of many arsenolipids in fish and algae, reversed-phase HPLC has been combined with ICP-MS and ESI-MS. Khan and Francesconi investigated the stability of three arsenolipids (arsenic fatty acids, AsFA-362 and AsFA-388, and arsenic hydrocarbon AsHC-332), common constituents of fish and algae, relevant to sample storage and transport, and to their preparation for quantitative measurements.<sup>45</sup> High performance liquid chromatography/electrospray triple quadrupole mass spectrometry (HPLC/ESI-MS) was used for arsenolipids analyses. The authors noted that although previous investigations of arsenolipids, focussing on their identification, have used hybrid instruments with accurate mass capability such as Q-TOF or Q-Orbitrap, the low-resolution triple quadrupole mass spectrometric system used in their study was perfectly suited: the precursor ion mode provided high selectivity, low LODs (0.002 ppb), and stable responses over long analysis times (RSD 3.6% over a 24 h run-time). Arroyo-Abad *et al.* separated six arsenolipids, AsB, and two unidentified As compounds in 60 minutes using a C18 column and a linear gradient elution from



100% A (0.1% formic acid in water) to 100% B (0.1% formic acid in methanol).<sup>46</sup> Viczek *et al.* used a C18 column to separate five arsenic-containing phosphatidylcholines using a gradient elution of 100% A (0.1% formic acid in water) to 100% B (0.1% formic acid in methanol).<sup>47</sup>

**2.2.4. Hydrophilic interaction liquid chromatography (HILIC).** HILIC is a normal phase chromatography technique that employs an aqueous mobile phase that is normally suited for reversed-phase chromatography. A layer of water from the mobile phase coats the hydrophilic stationary phase, and analytes are maintained either by partitioning into the water layer or by adsorption onto the polar stationary phase. Because the stationary phase is polar, HILIC can separate neutral, cationic, and anionic species all at once. This is especially useful for analyses of arsenic speciation, because any of these kinds of species could exist. There aren't many instances of HILIC being utilised for arsenic speciation, despite the fact that it offers a great potential for separating more arsenic species in a single analysis. Nine organoarsenicals were effectively discovered by Xie *et al.* using a zwitterionic HILIC column and ICP-MS/ESI-MS detection.<sup>48</sup> Frensemeier *et al.* employed HILIC to separate thirteen arsenicals in their research of Roxarsone electrochemical transformation products.<sup>49</sup> Lee *et al.* used a Luna HILIC column with an isocratic elution, containing 90% acetonitrile and 10% of 50 mM ammonium formate (pH 3), followed by ESI-MS for the specific detection of AsB in oyster.<sup>50</sup>

**2.2.5. Size exclusion chromatography (SEC).** Size exclusion chromatography, also known as gel filtration chromatography, is a chromatographic method that separates molecules based on their particle size. The gel consists of spherical beads containing pores of a specific size distribution. Separation occurs when molecules of different sizes are included or excluded from the pores within the matrix. The stationary phase in SEC is porous microbeads that separate analytes based on their size. Larger molecules are unable to travel through the small pore sizes and therefore elute faster than smaller molecules that take a longer path by going through the small pores of the stationary phase. SEC is not useful for speciation analysis of small arsenic compounds as the size difference between many arsenic species is minimal and cannot be resolved on an SEC column.

However, SEC is very effective for analysis of arsenic interactions with large molecules. For instance, analysis of arsenic-protein binding commonly uses SEC to separate protein-bound arsenic from free arsenic.<sup>12</sup> García-Sevillano *et al.* used SEC to measure arsenic-biomolecule complexes from liver extracts of *Mus musculus*.<sup>51</sup> Chen *et al.* used SEC to separate and collect protein-bound arsenic from free arsenic, followed by hydrogen peroxide treatment to release the protein-bound arsenic.<sup>52</sup> Schmidt *et al.* simultaneously measured binding of phenylarsine oxide to five different peptides and proteins (glutathione, oxytocin, aprotinin,  $\alpha$ -lactalbumin, thioredoxin) using SEC-ESI-MS.<sup>53</sup> Yang *et al.* investigated the roles of dissolved organic matter on arsenic mobilisation and speciation in environmental water using (SEC), combined with (ICP-MS), as well as three-dimensional excitation-emission matrix (3DEEM) fluorescence spectroscopy coupled with parallel factor analysis (PARAFAC). Low LODs (0.014–0.041 ppb) were reported.<sup>54</sup> The relevant literature on the chromatographic technique is summarised in the Table 2.

Hyphenated techniques have become more popular in recent times. Chromatographic methods such as liquid chromatography offer excellent possibility for the separation of all arsenic species because a variety of separation modes can be employed, followed by detection with different detection techniques, particularly in HPLC coupled in hyphenated techniques such as HPLC-hydride generation atomic absorption spectrometry (HG-AAS), hydride generation atomic emission spectrometry (HG-AES) and HPLC-ICP-MS. These methods are successfully and extensively used for the determination of the arsenic species at trace levels in environmental samples because of their low LODs.

HPLC methods for arsenic speciation are based on reversed phase chromatography with, usually, phosphate buffered mobile phases. This is relatively easy to set up, reasonably sensitive and provides the necessary chromatographic resolution of the target species. However, the need for a buffered, sometimes multi-component mobile phase leads to extra preparation work and more cost. In addition, the presence of phosphate in the mobile phase is not ideal for the ICP-MS instrument, as phosphates cause pitting of the interface

**Table 2** Examples of the most commonly used chromatographic techniques for arsenic determinations with some necessary details summarised including LOD, column used, analyte type and the relevant references

Techniques	Analyte	Column	LOD (ppb)	Reference
AE-HPLC	As(III), As(V), MMA, DMA, AsA	Shodex RSpak NN-614 column (150 × 6 mm)	0.20–0.80	55
CE-HPLC	AsB, DMA	Spheris S5SCX	0.20–0.33	39 and 56
IPC	As(III), As(V), MMA, DMA, AsB, AsC, TMAO, TMA, arsenosugar X	Capcell pak C18	0.04–0.07	42
RP-LC	Arsenolipids	Asahipak reversed-phase C-8 column (4.6 × 150 mm, particle size 5 $\mu$ m)	0.002	45
HILIC	Rox, PAA, ASA, PAO, DMA, MMA, AsB, AsC, TMAO	SeQuant ZIC-HILIC	10	48
SEC (SEC-ICP-MS)	As(V), As(III), AsB, DOM-As(III), MMA, DMA	Shodex OHPak SB-802.5 HQ	0.014–0.041	57



cones, leading to more frequent replacement or necessitating the use of more robust (and much more expensive) Pt-tipped cones. Longer term operation of HPLC methods for arsenic speciation eventually leads to a drop off in sensitivity and peak retention time drift caused by other components in the sample, leading to the need to periodically change the HPLC column. For lower numbers of samples, HPLC is a cost-effective solution, but the less expensive instrument cost can eventually be offset by the higher column consumable costs in the longer term.<sup>42</sup> In contrast, IC offers the benefits of sharp peak shapes (even for late eluting species), retention time stability, column robustness, excellent long-term peak area/height reproducibility and simpler mobile phases; only dilute ammonium carbonate is required, which is easy to prepare. In addition, dilute

ammonium carbonate is fully converted to gaseous species in the plasma ( $\text{NO}_2$ ,  $\text{H}_2\text{O}$  and  $\text{CO}_2$ ), so no damage or blocking of the interface cones occurs when using this mobile phase. Although not so much of an issue for arsenic speciation, IC also provides a metal-free sample path as standard, which provides lower backgrounds for other elements of speciation interest, such as chromium. Although IC instruments can be more expensive to purchase than HPLC systems, over time this can be offset by the lower consumables cost. Ponthieu *et al.* proposed a cation exchange IC-ICP-MS method for the simultaneous determination of eight arsenic species using mobile phases prepared from ammonium nitrate.<sup>58</sup> The relevant literature on the coupled/hyphenated chromatographic technique is summarised in the Table 3.

**Table 3** Summary of coupled chromatographic techniques describing separation/column, detector and analyte arsenic species

Separation process	Column	Detector	Arsenic species	Ref.
Anion exchange	Hamilton PRP-X100	ICP-MS	As(III), AsB, DMA, MMA, As(V), AsA, Rox	59
	Hamilton PRP-X100S	ICP-MS/ESI-MS	As(III), AsB, DMA, MMA, methyl-3AHPAA, As(V)	59
	IonPac AS7	ICP-MS	As(III), PAO, PAA, As(V), <i>o</i> -APAA, Rox, AsA	59
	Shodex RSPak NN-614	ICP-MS	As(V), MMA, As(III), PhAs, Rox, PhAsO, TMAO	59
	Dionex AS15A	ICP-MS	iAs, DMA, MMA, 4NPAA	59
	Hamilton PRP-X100	ICP-MS	As(III), As(V), DMA, MA, As-sug-PO <sub>4</sub> , As-sug-SO <sub>3</sub> , As-sug-SO <sub>4</sub>	60
	Hamilton PRP-X100	ICP-MS/ESI-MS	As-sug-PO <sub>4</sub> , As-sug-SO <sub>3</sub> , As-sug-SO <sub>4</sub> , As-sug-OH aglycone-free sugar	60
	Hamilton PRP-X110S	ICP-MS/ESI-MS/MS	AsB, As(V), Rox, NAHAA, MMA, DMA, As(III)	61
	Hamilton PRP-X110S	ICP-MS/ESI-MS/MS	AsB, N-AHAA, 3-AHPAA, As(III), As(V), MMA, DMA, Rox	54
Cation exchange	Spheris S5SCX	ICP-MS	Rox, methyl-Rox, methyl-3-AHPAA, methyl-N-AHPAA, AsB, As(III), DMA, MMA, As(V), 3-AHPAA, N-AHPAA	62
	IonoSpher 5C	ICP-MS	AsB, DMA	56
	Zorbax 300-SCX	ICP-QqQMS	As(V), As(III), DMA, TMAO	40
Reversed-phase	Asahipak C8	ICP-MS/ESI-QqQ	AsB, TMAO, TMAP, AsC, TMA	63
	ACE C18	ICP-MS/ESI-MS	AsFA (C <sub>17</sub> H <sub>35</sub> AsO <sub>3</sub> , C <sub>19</sub> H <sub>37</sub> AsO <sub>3</sub> ), AsHC (C <sub>17</sub> H <sub>37</sub> AsO)	45
Ion pair	Atlantis dC18	ICP-MS/ESI-qTOF-MS	As-sug-OH, As-sug-PO <sub>4</sub> , As-sug-SO <sub>3</sub> , AsPL (C <sub>44</sub> H <sub>87</sub> AsO <sub>14</sub> P, C <sub>45</sub> H <sub>89</sub> AsO <sub>14</sub> P, C <sub>46</sub> H <sub>91</sub> AsO <sub>14</sub> P, C <sub>47</sub> H <sub>93</sub> AsO <sub>14</sub> P, C <sub>47</sub> H <sub>87</sub> AsO <sub>14</sub> P, C <sub>45</sub> H <sub>85</sub> AsO <sub>14</sub> P, <i>etc.</i> ), AsHC (C <sub>17</sub> H <sub>37</sub> AsO, C <sub>18</sub> H <sub>39</sub> AsO, C <sub>19</sub> H <sub>41</sub> AsO, C <sub>20</sub> H <sub>43</sub> AsO, C <sub>21</sub> H <sub>45</sub> AsO, C <sub>22</sub> H <sub>47</sub> AsO), AsFA (C <sub>22</sub> H <sub>35</sub> AsO <sub>3</sub> , C <sub>22</sub> H <sub>37</sub> AsO <sub>3</sub> )	64
	Capcell pak C18	ICP-MS/ESI-qTOF-MS	AsFA (C <sub>10</sub> H <sub>21</sub> AsO <sub>3</sub> , C <sub>11</sub> H <sub>21</sub> AsO <sub>3</sub> , C <sub>13</sub> H <sub>23</sub> AsO <sub>3</sub> , C <sub>15</sub> H <sub>31</sub> AsO <sub>3</sub> )	46
	Shim-pack VP-ODS C18	ICP-MS	As(III), As(V), MMA, DMA, AsB	42
	Agilent ZORBAX SB-Aq	ICP-MS	As(III), As(III), MMA, DMA, TMAO, TMA, AsB, AsC	65
HILIC	Thermo Fisher Trinity P2	ICP-MS	As(III), As(V), MMA, DMA	43
	Phenomenex HILIC	ESI-MS/MS	Rox, As(V)	49
Size exclusion	Phenomenex	ICP-MS/ESI-MS/MS	AsB	50
	Shodex OHpak SB-802.5 HQ	ICP-MS	As(III), As(V), MMA, DMA, TMAO, MMTA, DMMTA	52
Others	GO@SiO <sub>2</sub>	ICP-MS	As(V), As(III), AsB, DOM-As(III), MMA, DMA	57
	Sigma-Aldrich	ICP-MS	As(III), DMA, MMA, As(V)	66
	Discovery HS F5	ICP-MS	As(III), As(V), MMA, DMA	67 and 68



Table 4 Comparison of arsenic kit based on Gutzeit method

Commercial colorimetric kit	Theoretical LOD (ppb)	Practical LOD (ppb)	Reliability (ppb)	Cost per sample (USD)	Time per sample (min)	Features	Data/signal type	Ref.
NIPSOM	10	>20	Unreliable <70	0.4	5	Colour sensitivity to yellow; working quickly	Colour change (range)	70 and 72
Merck	10	>50	Unreliable <70	0.5–1.00	30	Colour sensitivity to yellow; working quickly	Colour change (range)	69, 70 and 72
GPL	10	NA	Unreliable <70	0.4	20	Colour sensitivity to yellow; working quickly	Colour change (range)	70
AAIH & PH	50	>50	Unreliable <70	0.4	NA	Colour sensitivity to yellow; working quickly	Colour change (binary)	70 and 72
AAN	10	>20	Unreliable <70	0.4	30	Colour sensitivity to yellow; working quickly	Colour change (range)	69, 70 and 72
Quick As	5	NA	Can identify samples > 15	1.00–2.00	NA	Colour sensitivity to yellow; working quickly	Colour change (range)	73
Hach Ez	10	NA	Can identify samples > 15	<1–2.00	20–40	Colour sensitivity to yellow; working quickly	Colour change (range)	69 and 73
Arsenator	0.5–2	NA	Found to be correct 85% of the time, more reliable at lower concentrations	1.00	20	Ability to make accurate dilutions	Digital readout	69 and 74

### 2.3. Colorimetric methods

Colorimetry and spectrophotometry are techniques used to identify molecules depending on their absorption and emission properties. Colorimetric methods are desirable for portable arsenic monitoring because of the simplicity of the detection method. As with the traditional field kits, detection can be carried out by the human eye or digital imaging can be used for more sophisticated analyses. An advantage of colorimetry with respect to field determinations is that several digital detection instruments are portable; for example, a camera, UV-Vis spectrometer, or smartphone can be used as a digital detector. In order to enhance user-friendliness, different devices have been exploited for custom-designed microfluidic system. The main difference between colorimeter and spectrophotometer is that colorimeter is a device which measures absorbance of specific colours, whereas a spectrophotometer measures transmittance or reflectance as a function of wavelength. In other words, colorimetry uses fixed wavelengths that are in the visible range while spectrophotometry can use wavelengths in a wider range. A spectrophotometer has high precision and increased versatility and more suitable for complex colour analysis because it can determine the spectral reflectance at each wavelength. However, spectrophotometers are costlier than colorimeters.

**2.3.1. Marsh reaction & Gutzeit method.** The Gutzeit method is based on the reaction of arsine gas ( $\text{AsH}_3$ ) with mercuric bromide ( $\text{HgBr}_2$ ). LODs of 10 ppb are possible by visual comparison of the coloured stain with a colour

calibration.<sup>69</sup> The typical test kit analysis is based on the Gutzeit modification of the Marsh reaction. Marsh test was invented by James Marsh in 1836. Gutzeit modified it in 1879 and since then this method has been widely used for more than a century for the detection of Arsenic. The Gutzeit method is the most commonly used approach for colorimetric arsenic analysis and employed to develop arsenic field test kits. Although the Gutzeit method based technique is economical, it produces toxic arsine gas as by-products.<sup>16</sup> A recent development of the Gutzeit's method is the arsenic field-testing kits. However, the kits failed in a high fraction (up to 68%) when groundwater samples were analysed.<sup>70,71</sup> Yogarajah *et al.* have summarised and compared all the relevant Gutzeit method based Arsenic Kits in a single table.<sup>11</sup> The relevant literature about the commercial kits based on Gutzeit method are summarised in the Table 4.

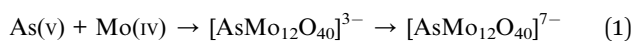
**2.3.2. Molybdenum blue based method for arsenic(v).** Like the Gutzeit method used by existing test strips, another colorimetric reaction for arsenic detection is the molybdenum blue assay. This assay consists of the reaction between arsenate and molybdenum to give a coloured heteropolyacid ion product. Conducting the molybdenum blue reaction essentially involves passive flows and mixing, so this process can be microfluidically adapted. However, a potential drawback is interference from phosphates and silicates which compete with arsenic and react with molybdenum. Since phosphate and silicate levels of natural waters are typically much higher than the amount of arsenic present, they must be removed from solution before



**Table 5** Colorimetric/spectrophotometric techniques for the determination of arsenic in water

Techniques	Detection time	Portability	LOD (ppb)	Reference
Molybdenum blue	>30 min	Not portable, bulky instrument	1–15	81
Methylene dye	~6 min	Potentially portable	10–100	82
Sulphanilic acid – NEDA	~30 min	Portable	18	79 and 83
Paper based	Very quick	Portable	1	80 and 84

analysis.<sup>11,75</sup> Arsenate (As(v)) and molybdate in solution react to form an  $\alpha$ -Keggin arsenomolybdate heteropolyacid, followed by reduction to heteropoly blue, serving as the basis for colorimetric determination (eqn (1)). Since arsenite (As(III)) does not react with molybdate, it needs to be oxidised to As(v) to form the colour complex for detection.<sup>76</sup>



**2.3.3. Methylene blue dye.** An alternative colorimetric reaction for arsenic detection is based on the direct interaction between arsenic and the cationic organic dye methylene blue. When reduced by arsine gas, methylene blue becomes colourless. The rate of reaction can be promoted when catalysed within an anionic micelle in the presence of silver nanoparticles, which serve to facilitate the electron relay from arsine gas to the dye.<sup>77</sup> Instead of estimation, a numeric reading of As concentration can be obtained by the digital reader.

To avoid human bias, digital colour processing can replace semi-quantification by visual comparison with a colour chart. Such an idea was adopted by a number of commercial products, for instances, the Arsenator by Wagtech and the DigiPAS by Palintest. Parts used to remove interfering gas, such as hydrogen sulphide, are included in modern kits. A recent evaluation of 8 commercial arsenic field test kits for drinking water (Bangladesh) by comparing with HG-AAS showed a performance correlation with the product price. The two most expensive kits, LaMotte and Quick II kit, provided the best estimates while the cheapest were neither accurate nor precise.<sup>78</sup>

**2.3.4. Sulphanilic acid – NEDA.** Another colorimetric method for arsenic detection is the reaction presented by Sharma *et al.* using sulphanilic acid and *N*-(1-naphthyl)ethylene diamine dihydrochloride (NEDA).<sup>79</sup> Here, arsenic(III) in solution first reduces the sulphanilic acid; the resultant product then goes on to react with NEDA to produce a magenta-coloured product.

**2.3.5. Paper-based sensors.** Paper-based methods have been used in analytical detections for thousands of years. Nath *et al.* have developed a portable paper-based sensor for arsenic detection, by using modified gold nanoparticles.<sup>80</sup> Their rapid, ultrasensitive Y-shaped design is specific for As(III), and can detect arsenic concentrations down to 1 ppb.

Some of the relevant literature on the colorimetric arsenic detection technique is summarised in the Table 5.

A colorimetry based, semi-automated portable sensor device has been developed for the detection of total inorganic arsenic (As(III) and As(v)) in drinking water. Authors claimed that the response for total inorganic arsenic is linear in the range 5–20 ppb with a sensitivity of 1 ppb.<sup>13</sup> The effect of elevated temperature (of water sample) on the kinetics and performance of the device was also interrogated to reduce the measurement time. Costa and Maniruzzaman recently reported the ‘detection of arsenic contamination in drinking water using colour sensor’.<sup>15</sup> An arsenic detection kit and simple colour sensor was used to develop their system to detect the arsenic percentage in water.

According to authors, the results reflect that different arsenic contamination produces different intensities of colour, thereby can be used to distinguish between different arsenic percentages. However, the method may not be fully reliable as it depends on visual colour comparison.<sup>15</sup>

Silver nanoparticles (AgNPs) are reported to provide a rapid response to localised surface plasmon resonance compared to gold nanoparticles with enhanced sensitivity.<sup>85</sup> Polyethylene glycol (PEG)-functionalised silver nanoparticles are well-suited for detecting arsenic(III) ions in an aqueous medium.<sup>86</sup> The PEG-modified silver nanoparticles are sufficient enough to detect arsenic(III) in 1 ppb due to the addition of PEG. PEG-functionalised AgNPs have adjustable negative surface charges, responsible for the nanoparticle’s stability and the electrostatic repulsion between negatively charged surfaces of AgNPs protects them from agglomeration. Interestingly, in the presence of As(III), the functional AgNPs interacted with PEG hydroxyl groups, which led to the aggregation of AgNPs. As a result, the colour of functionalised nanoparticles changed from yellow to bluish (Fig. 6). A silver nanoprisms (AgNPr) based assay has been designed and reported to achieve the wide range morphologically modified surface plasmon tuning–detuning for accurate colour-coded detection and sensing of As(III) over other alkali, alkaline, and transition metals (Fig. 7).<sup>87</sup> Plasmon tuning–detuning not only confirms the presence but also can detect As(III) concentration up to a limit of 75 ppb. The authors

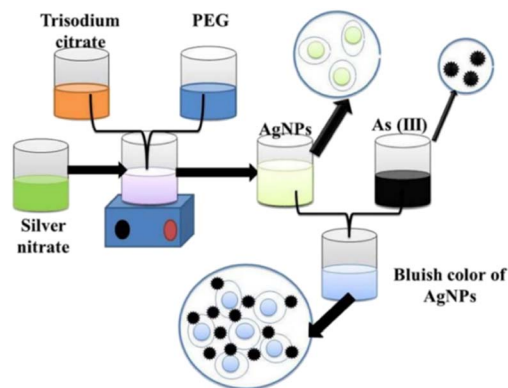


**Fig. 6** Functionalised silver nanoparticles as an effective medium towards trace determination of arsenic(III) in aqueous solution<sup>86</sup> (reprinted from ref. 86; Copyright (2019), with permission from Elsevier).



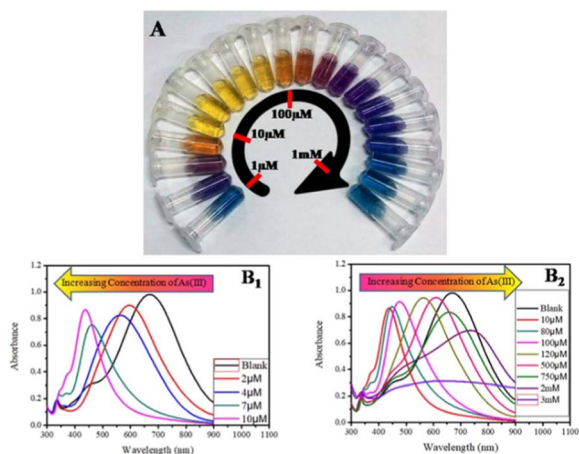


Fig. 7 (A) Concentration-dependent colour-coded sensing of arsenic(III) between the concentration range of  $10^{-6}$  to  $10^{-3}$  M, (B) tuning of SPR as a result of morphological change of AgNPR (silver nanoprisms) at different concentrations of arsenic(III) between  $10^{-6}$  and  $10^{-3}$  M where (B<sub>1</sub>) shows the variation of plasmon band at different lower concentrations of arsenic(III) in the range of 0.0–10.0 μM (0.0 μM (blank): black trace ( $\lambda_{\text{max}} = 704$  nm), 1.0–2.0 μM: blue trace, 2.0–4.0 μM: orange trace, 5.0–7.0 μM: red-violet trace, 8.0–10.0 μM: blue-violet trace) and (B<sub>2</sub>) at different higher concentrations of arsenic(III). The plasmon band, and hence the colour of the nanomaterials, changes in a distinct manner, where a specific colour remains unchanged in a broader range of growing concentrations such as: 10.0–80.0 μM: yellow, 90.0–100.0 μM: orange, 110.0–200.0 μM: dark red, 250.0–500.0 μM: purple, 750.0 μM to 2 mM: different shades of blue, 3–10 mM: faded blue, and above 10 mM the colour becomes faint blue to grey or almost colourless<sup>87</sup> (reprinted with permission from ref. 87. Copyright [2019] American Chemical Society).

have suggested that the assays ability to detect As(III) in real water samples coupled with its cost effectiveness make it potentially useful for field applications.<sup>87</sup>

## 2.4. Biological methods

**2.4.1. Whole cell biosensors (WCBS).** Whole cell biosensors have been employed for detection of arsenic in drinking water. They have attracted considerable interests because they are robust, eco-friendly, and cost-effective.<sup>88</sup> For example, the *E. coli*-based ARSOLux biosensor kit has been successfully applied to field testing of As in groundwater. The ARSOLux kit costs around 1€ per test including labour. The cost may be further reduced by a factor of 5 to 10 if they are mass produced.<sup>89</sup> However, many reported biosensors often suffer from high background noise and limited in their sensitivity as well as dynamic range.<sup>90,91</sup>

Biological detection methods developed for arsenic have mostly been based on the *ars* operon. An operon is a cluster of genes which are transcribed together giving a single messenger RNA (mRNA) molecule that encodes for multiple proteins.<sup>92</sup> Plasmid encoded *ars* operons found in bacterial species such as *E. coli* are known to confer a certain level of resistance to As(III) and As(V) through giving cells the ability to remove As species from within the cell, lowering the intracellular concentration of toxic arsenic species.<sup>93</sup> Upon encountering arsenite, a dedicated

sensory protein in the bacterial cell called ArsR will undergo a conformational change that unleashes expression of the defence system.<sup>94</sup> This protein functions as a transcriptional repressor, attaching to a particular DNA sequence (the operator) that overlaps the binding site for RNA polymerase in the absence of arsenic (the promoter). However, when binding arsenite, ArsR will lose its affinity for the DNA and RNA polymerase can start transcription.<sup>94</sup> This detoxification system can be exploited for highly specific and sensitive arsenic detection. Modifications involve the coupling of the regulatory elements of the *ars* operon, including the transcriptional regulator and cognate promoters to reporter genes for Green fluorescent protein (GFP), luciferase, and  $\beta$ -galactosidase (lacZ). In response to the presence of arsenic, genetically modified bacterial species such as *E. coli*, *Bacillus subtilis*, *Staphylococcus aureus*, and *Rhodospseudomonas palustris*, generate reporter proteins, the amount or activity of which is related to arsenic concentration. Such an approach has allowed for LODs in the order of 1 ppb. E. Diesel *et al.* (Fig. 8) summarised the use of

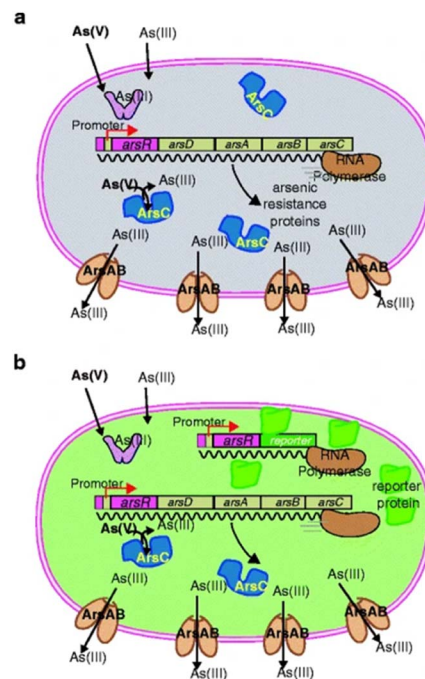


Fig. 8 Design principle of most bacteria sensor-reporters for arsenic: (a) when no arsenic enters the cell, the ArsR protein represses the transcription of the arsenic defence system genes (*arsD*, *arsC*, *arsA*, and *arsB*) from one particular DNA region upstream of the gene for itself (the operator–promoter site). In the presence of arsenite in the cell, ArsR loses affinity for the operator and RNA polymerase will transcribe the *arsDCAB* genes to produce the defence. ArsC is a reductase that reduces arsenate [As(V)] to arsenite [As(III)], whereas ArsAB constitute an efflux pump for arsenite. (b) In the sensor–reporter strain, an extra copy of the operator–promoter DNA fused to the *arsR* gene and a gene for a reporter protein is added to the cell. In this case, when arsenite or arsenate is sensed by the cell, transcription for the reporter gene will also be unleashed and the reporter protein will be formed. The presence or activity of the reporter protein is subsequently measured<sup>95</sup> (reprinted by permission from Springer [ref. 95] COPYRIGHT (2009)).



bacteria-based assays as an emerging method that is both robust and inexpensive for the detection of arsenic in groundwater for both in the field and laboratory.<sup>95</sup>

Kaur *et al.* mentioned that the development of whole cell biosensors employing these metabolic processes for their design.<sup>96</sup> In case of arsenic, the well-established ability of As(III) or As(V) to bind the ArsR protein and undo its repressor function on the Ars promoter leads to subsequent synthesis of reporter genes. Thus, whole-cell-based biosensors devised using the above approach have been further subdivided, based on their signal transduction mechanisms like luciferase, lacZ and GFP whereby the signal relay is either in terms of fluorescence, luminescence or colorimetry as depicted in Fig. 9A.<sup>96</sup> Wang *et al.* developed a convenient analysis method for environmental monitoring, that intended to employ *in vitro* protein expression technology to detect toxic pollutants based on evolved genetically encoded biosensors (Fig. 9B). His team established a genetically encoded biosensor *in vitro* with ArsR and GFP reporter gene. Given that the wildtype ArsR did not respond to arsenic and activate GFP expression *in vitro*, they found, after screening, an evolved ArsR mutant ep3 could respond to arsenic and exhibited an approximately 3.4-fold fluorescence increase.<sup>97</sup>

The engineered promoter modification approach is used to improve the performance of whole-cell biosensors to facilitate their practical application. A recent study, demonstrated how to design the core elements (*i.e.*, RNA polymerase binding site and transcription factor binding site) of the promoters to obtain a significant gain in the signal-to-noise output ratio of the whole-cell biosensor circuits (Fig. 10, left).<sup>88</sup> The arsenite-regulated promoter from *Escherichia coli* K-12 genome was modified to lower background and higher expression and was achieved by balancing the relationship between the number of ArsR binding sites (ABS) and the activity of the promoter and adjusting the location of the auxiliary ABS. A promoter variant ParsD-ABS-8 was obtained with an induction ratio of 179 when induced with 1  $\mu\text{M}$  arsenite (11-fold increase over the wild-type promoter). The reported biosensor exhibited good dose-

response in the range of 0.1 to 4  $\mu\text{M}$  ( $R^2 = 0.9928$ ) of arsenite with a detection limit of *ca.* 10 nM.

An arsenic WCB with a positive feedback amplifier *Escherichia coli* DH5 $\alpha$  was developed and reported (Fig. 10, right),<sup>98</sup> where the output signal from the reporter mCherry was significantly enhanced by the positive feedback amplifier. The sensitivity of the WCB with positive feedback was about 1 order of magnitude higher compared to without positive feedback when evaluated using a half As(III) concentration (half-saturation). The LOD for As(III) was reduced by 1 order of magnitude to 0.1  $\mu\text{M}$ , lower than the WHO standard for the arsenic levels in drinking water (0.13  $\mu\text{M}$ ). The WCB with the positive feedback amplifier exhibited exceptionally high specificity toward As(III) when compared with other metal ions. The importance of genetic circuit engineering in designing WCBs, and the use of genetic positive feedback amplifiers may be a good strategy to improve the performance of WCBs. The integration of WCBs for the field-ready electrochemical detection of arsenic (FRED-As) has been reported recently.<sup>99</sup> Sergio Sánchez *et al.* reported a WCB biosensor which was followed by electrochemical measurements and provided enhanced accuracy and signal intensity compared to traditional bacterial-detection approaches (Fig. 11). FRED-As had a number of benefits including ease of use, potential for measuring a wide spectrum of metals, sensitivity *etc.* When integrated within a customised hardware system, the reported whole-cell biosensor demonstrated excellent specificity and sensitivity with an LOD 95% confidence, (FRED-As) of 2.2 ppb As(III).<sup>99</sup> This sensitive and easy-to-use approach may be a viable alternative for on-site arsenic testing.

**2.4.2. Biomolecules related biosensors (aptasensors).** Most biomolecules-based biosensors are still in early stage of development without demonstrated on-site applications. Mao *et al.* in their review article nicely summarised the performance of the fluorescent and colorimetric aptasensors which is presented in Fig. 12 and discussed.<sup>100</sup> The first arsenic fluorescent aptasensor paper was published in 2014, describing a DNA-based biosensor for arsenate detection using DNA adsorption by magnetic beads

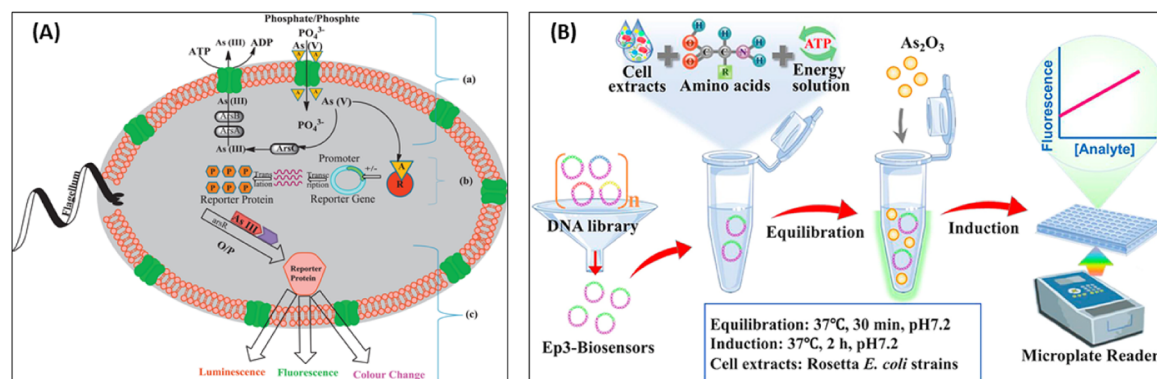


Fig. 9 (A) Schematic representation of whole-cell-based biosensor for (a) arsenic [As(V) and As(III)] transport by phosphate channel, (b) working mechanism of signal transducer for arsenic biosensor, and (c) detection of As(III) by luminescence, fluorescence and colour change (for interpretation of the references to colour in this scheme legend, the reader is referred to the web version of this article)<sup>96</sup> (reprinted from ref. 96; Copyright (2015), with permission from Elsevier). (B) Arsenic detection with genetically encoded biosensors *in vitro*. Schematic of arsenic induction reaction<sup>97</sup> (reprinted from ref. 97; Copyright (2021), with permission from Elsevier).



(Fig. 12A).<sup>101</sup> Magnetic beads adsorbed fluorescently-labeled oligonucleotides through the phosphate backbone resulting in fluorescence quenching. In the presence of arsenate, the adsorbed oligonucleotides were displaced due to higher affinity towards arsenate resulting in increased fluorescence. This biosensor had an LOD of as low as 300 nM (arsenate). Notably, this assay was a novel way to use DNA for target recognition through its phosphate backbone instead of the bases. Oroval *et al.* used the combination of mesoporous silica nanoparticles with aptamers and designed a novel fluorescence sensor for As(III) determination spanning a dynamic range from 53.2 to 798 nM with a LOD of 11.97 nM (Fig. 12B).<sup>102</sup> The pores of the inorganic support were modified by rhodamine B followed by the external surface functionalisation with amino-propyl moieties. The final capped solid was made *via* the introduction of the aptamer. When arsenic (As(III)) was introduced, it would induce unblocking of the pores by displacement of the aptamer from the surface of mesoporous silica nanoparticles with subsequent dye delivery. Compared to the other potential nanomaterials used in sensing protocols, mesoporous silica nanoparticles are one of the most promising supports because of their remarkable properties such as high inner surface area, facile functionalised with (bio) chemical or supramolecular ensembles and flexible surface-modification chemistry.

Ensafi *et al.*, have developed a CdTe/ZnS QDs (quantum dots) aggregation-based fluorimeter aptasensor for As(III) (Fig. 12C).<sup>103</sup> The aptamer was designed to aggregate cationic cysteamine-stabilised CdTe/ZnS QDs, which led to fluorescence quenching. When As(III) was introduced, the complex between the aptamer and As(III) prevented aggregation of the QDs. Therefore, depending upon the As(III) concentration, the QDs fluorescence was enhanced due to de-aggregation. The

fluorescence analysis held a promising LOD of 1.3 pM with a dynamic range of  $10^{-2}$  to  $10^3$  nM. The proposed QDs based aptasensor has advantages such as high sensitivity and selectivity, compared with conventional dyes based aptasensors. Zhang *et al.* (Fig. 12D), reported an arsenite detection strategy based on the fluorescence enhancement of DNA QDs.<sup>104</sup> In their work, they synthesised DNA QDs using G/T-rich ssDNA that showed special optical properties, and acquired the basic structure and biological activities of ssDNA precursors, making the QDs selectively bind with arsenite, driving the (GT)<sub>25</sub> region towards conformational switching and form a well-ordered assembly. They speculated that the strong inter-molecular interaction and efficient stacking of base pairs stiffened the

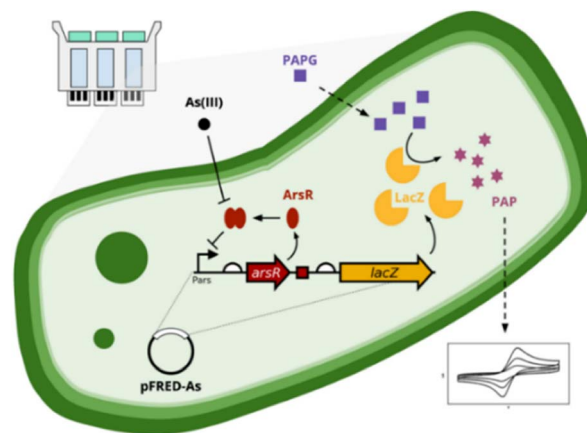


Fig. 11 Process schematic of the bacterial biosensor system used for arsenic detection<sup>99</sup> (reproduced from ref. 99; Copyright (2021), with permission from IOP Publishing).

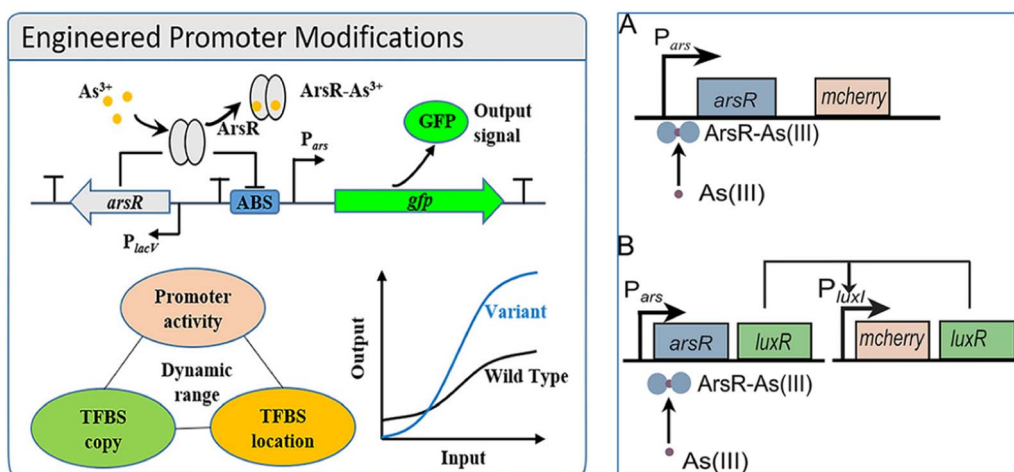


Fig. 10 Left: Design and improvement of arsenic biosensors (engineered promoter modifications): construction of arsenic responsive biosensor genetic circuit<sup>88</sup> (reprinted with permission from ref. 88. Copyright [2019] American Chemical Society). Right: Schematic of the arsenic WCBs with positive feedback (B) and without (A). (A) The typical arsenic WCB consists of the ArsR-regulated promoter  $P_{ars}$ , the regulator *arsR*, and the reporter gene *mCherry*. (B) The positive feedback WCB consists of the *arsR*- $P_{ars}$  regulatory circuit and a positive feedback amplifier where *LuxR* from the  $P_{luxI}$  promoter activates its own expression and forms a positive feedback loop<sup>98</sup> (reprinted with permission from ref. 98. Copyright [2019] American Society for Microbiology).



assembly structure, blocked non-radiative relaxation channels, populated radiative decay, and thus made the assembly highly emissive as a new fluorescence center. The fluorescence enhancement induced by arsenite promoted QDs as light-up probes for determination of arsenite. A very good linear relationship was demonstrated between fluorescence intensity and logarithmic arsenite concentration from 1–150 ppb with an LOD of 0.2 ppb reported.

The first colorimetric arsenic aptasensor was reported by Wu and co-workers (Fig. 12E). In the presence of Arsenic, the aptamer selectively interacted with As(III) forming an As-aptamer complex. The formation of this complex allowed the cationic polymer poly-diallyldimethylammonium (PDDA) to

aggregate AuNPs, resulting in an obvious colour variance allowing for highly sensitive colorimetric arsenic detection.<sup>105</sup> In the same year, Wu and co-workers reported another aptasensor employing a different polymer (cetyltrimethylammonium bromide, CTAB) that also utilised AuNP induced aggregation for As(III) detection (Fig. 12F). The dynamic range spanned from 1–1500 ppb with the LOD of 0.6 ppb for colour analysis and 40 ppb for naked-eye detection, respectively.<sup>106</sup> Following the same strategy, Nguyen *et al.* developed a novel biosensor based on CTAB and AuNPs for colorimetric detection of As(III) with an LOD of 16.9 ppb in real samples.<sup>14</sup> Zhou's group (Fig. 12G) reported the salt-induced aggregation of AuNPs (classical aptamer-based AuNPs colorimetric method) for As(III)

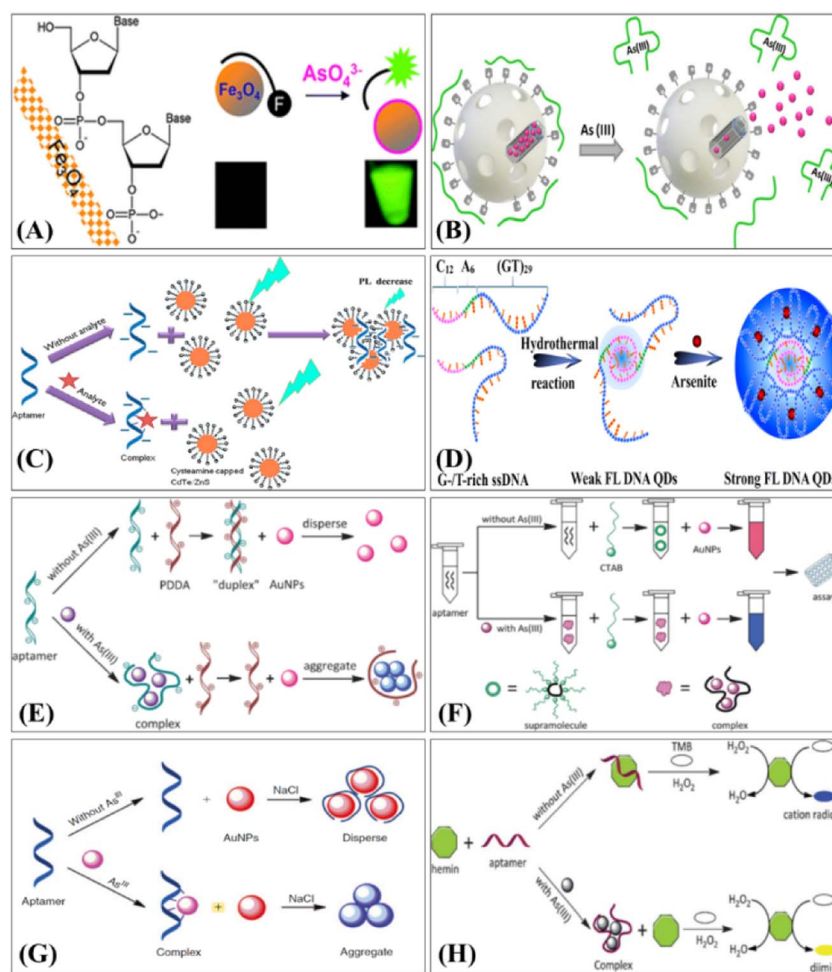


Fig. 12 Principles of representative fluorescence-based arsenic aptasensor: (A) DNA adsorption by magnetic iron oxide nanoparticles and its application for arsenate detection<sup>101</sup> (reproduced from ref. 101 with permission from Royal Society of Chemistry, copyright [2014]). (B) Fluorescence aptasensors of As(III) using silica nanoparticles<sup>102</sup> (reprinted with permission from ref. 102. Copyright [2017] American Chemical Society). (C) The fluorescence quenching analysis<sup>103</sup> (reprinted from ref. 103; Copyright (2016), with permission from Elsevier). (D) The fluorescence enhancement analysis based QDs aptasensor for arsenite determination<sup>104</sup> (reprinted from ref. 104; Copyright (2017), with permission from Elsevier). Principles of representative colorimetry-based arsenic aptasensor techniques: (E) Cationic polymers and aptamers mediated aggregation of AuNPs for colorimetric detection of As(III) in aqueous solution<sup>105</sup> (reproduced from ref. 105 with permission from Royal Society of Chemistry, copyright [2012]). (F) Ultrasensitive aptamer biosensor for As(III) detection in aqueous solution based on surfactant-induced aggregation of AuNPs<sup>106</sup> (reproduced from ref. 106 with permission from Royal Society of Chemistry, copyright [2012]). (G) Aptasensor for As(III) detection in aqueous solution based on cationic salt-induced aggregation of AuNPs<sup>107</sup> (reprinted from ref. 107; Copyright [2014]; with permission from CSIRO Publishing). (H) Regulation of hemin peroxidase catalytic activity by As-binding aptamers for colorimetric detection of As(III)<sup>108</sup> (reproduced from ref. 108 with permission from Royal Society of Chemistry, copyright [2013]).



detection.<sup>107</sup> In this study, an arsenic aptamer was employed as the probe with AuNPs as a colorimetric signal. When As(III) was absent in the solution, AuNPs were wrapped by aptamer and therefore stable even when a high concentration of sodium chloride was in the solution, showing a red colour. When introduced to As(III), the AuNPs were easy to aggregate due to the formation of the As-aptamer complex, showing a blue coloured solution. Through monitoring the colour variance, the rapid colorimetric detection methods for As(III) with a dynamic range from 1.26 to 200 ppb and a LOD of 1.26 ppb was demonstrated. However, AuNPs-based biosensors are dependent on salt-induced aggregation, which seems to make them more susceptible to interference by environmental matrices. Natural matrices are typically diluted in a buffer before sensing, but matrices with high salt concentrations must be handled carefully when performing this assay.

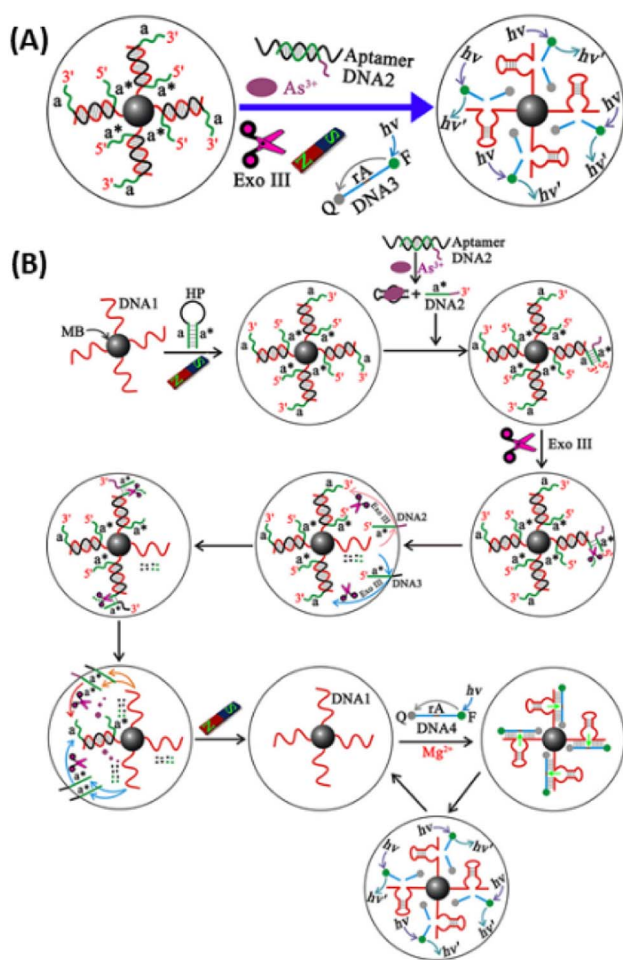


Fig. 13 (A) Highly sensitive aptasensor for trace arsenic(III) detection using DNAzyme as the biocatalytic amplifier. (B) Schematic illustration of the assay principle for As(III) detection based on target-triggered successive signal amplification strategy<sup>a</sup> (a domain a is complementary to domain a\*). The sequence of DNA1 corresponds to the Mg<sup>2+</sup>-dependent DNAzyme. MB, magnetic beads; HP, hairpin probe; Exo III, exonuclease III; F, fluorophore (FAM); Q, quencher (TAMRA)<sup>110</sup> (reprinted with permission from ref. 110. Copyright [2019] American Chemical Society).

Divsar *et al.*, (2015)<sup>109</sup> prepared AgNPs modified by aptamer (Apt-AgNPs) and used it for colorimetric determination of As(III). In their work, As(III) could selectively interact with Apt-AgNPs resulting in the formation of an As(III)-Apt-AgNPs complex and cause an obvious decrease in peak intensity ( $\lambda_{\text{max}}$  403 nm), which was proportional to As(III) concentration. Additionally, a combination of a central composite design optimisation method and response surface methodology was applied to optimize the efficiency of As(III) analysis. The linear range of the colorimetric biosensor held a wide scope of As(III) concentration from 50 to 700 ppb with a LOD of 6 ppb. Wu *et al.* reported the development of a colorimetric aptasensor for As(III) determination that was designed through the combination of aptamer and G-quadruplex DNAzyme (Wu *et al.* Fig. 12H).<sup>108</sup> The catalytic activity of hemin peroxidase was temporarily inhibited by As-aptamer complex. In the presence of As(III) an As-aptamer complex formed allowing hemin peroxidase catalyze TMB oxidation in the presence of H<sub>2</sub>O<sub>2</sub> resulting in an obvious increase of UV-vis spectra intensity (442 nm), LOD of 6 ppb was reported.

Recently, a highly sensitive fluorescence sensing platform for As(III) detection based on target-triggered successive signal amplification strategy was demonstrated. As(III) aptamer was used as the recognition unit and in the presence of As(III), the blocking DNA is released to trigger the cascade signal amplification process. The integration of Exo III-assisted DNA recycling and DNAzyme-based catalytic cleavage with multiple turnovers

Table 6 Some of the biological sensors with their performances from the relevant literature review

Biosensor specifications	Response time (min)	LOD (ppb)	As species detected	Reference
<i>E. coli</i> arsRp: luc	120	3.75	As(III)	111
<i>E. coli</i> DH5 $\alpha$ (pASPW2-arsR-luxCDABE)	120	0.74	As(III)	112
<i>E. coli</i> DH5 $\alpha$ (pPROBE'arsR-ABS-RBS-lacZ strain 2245) harboring arsR-lacZ fusion	4.23	0.8	As(III)	113
Magnetic nanoparticle based thermo-responsive biosensor	0.08	1	As(III)	114
<i>Rhodospseudomonas palustris</i> (crtIBS)	—	NA	As(III), As(V)	115
Aptamer-CTAB-AuNPs	3	16.9	As(III)	14
AuNPs DNA aptamer	65	161	As(III)	116
ssDNA-AuNPs	15	0.18	As(III)	117
Aptamers-AuNPs-surfactant	35	0.6	As(III)	106
<i>S. cerevisiae</i> pdr5 $\Delta$ luxAB gene construct	60	0.0007	As(V)	118
<i>A. niger</i> harboring arsA-egfp fusion protein	720	1.8	As(V)	119
<i>E. coli</i> strain 1598 harboring plasmid pPROBE-ArsR-ABS	72	10	As(III)	120
DNA functionalised SWCNT hybrid biosensor	180	0.05	As(III)	121
Calf thymus DNA based SPR biosensor	30	10	As(III)	122



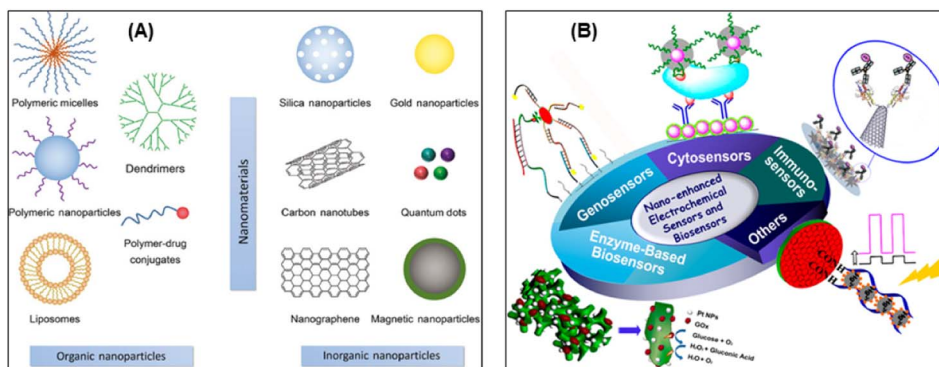


Fig. 14 (A) Different types of engineered nanomaterials divided into organic and inorganic nanomaterials<sup>123</sup> (reproduced with permission from ref. 123. Copyright [2017] Walter de Gruyter). (B) Schematic illustration of electrochemical sensors and biosensors based on nanomaterials and nanostructures, in which electrochemical sensors for small molecular, enzyme-based biosensors, genosensors, immunosensors, and cytosensors are demonstrated<sup>124</sup> (reprinted with permission from ref. 124. Copyright [2015] American Chemical Society).

results in the generation of amplified fluorescence signals (significantly) for highly sensitive quantification of trace levels of As(III), and a detection limit of 2 pM was achieved (Fig. 13).<sup>110</sup>

Some of the biological sensors with their performances are summarised in Table 6.

## 2.5. Electrochemical methods

**2.5.1. Nanomaterials & electrochemical sensor/biosensor fabrication.** Developments in nanotechnology have been beneficial to electrochemical analysis. Due to their unique chemical and electrical properties nanomaterials (nanotubes, metal nanoparticles, graphene, nanorods, quantum dots (QDs) and polymer nanocomposites) have the potential to improve sensitivity, selectivity and response of electrochemical sensors and biosensors (Fig. 14A).<sup>123</sup> Nanomaterial modified electrodes have several advantages including increased surface area, improved catalytic activity, increased electron transfer and excellent biocompatibility. With remarkable achievements in nanoscience and nanotechnology, nanomaterial-based electrochemical signal amplifications have great potential in improving both the sensitivity and selectivity for sensors and biosensors development. It is well-known that the electrode materials play a critical role in the construction of high-performance electrochemical sensing platforms for detecting target analyte molecules *via* the various analytical principles and mechanisms. Furthermore, in addition to electrode materials, functional nanomaterials not only produce a synergistic effect among catalytic activity, conductivity, and biocompatibility to accelerate the signal transduction but also amplify biorecognition events with specifically designed tags (signal), thereby leading to highly sensitive biosensing. Significantly, extensive research on the construction of functional electrode materials, coupled with numerous electrochemical methods, is advancing the wide application of electrochemical devices (Fig. 14B).<sup>124</sup>

As mentioned above, electrode surface modification with metallic nanoparticles, carbonaceous nanomaterials (*e.g.* carbon nanotubes, nanofibers and graphene) and even enzymes

(arsenite oxidase) can improve detection sensitivity and selectivity, while circumventing interferences. Fig. 15 shows the schematic comparing the laboratory based electrochemical devices *vs.* portable electrochemical devices and classical electrodes *vs.* screen-printed electrodes. The commonly used materials (textile, paper based *etc.*) and fabrication methods (inkjet, screen and 3D printing) are illustrated for the construction of flexible and wearable printed electrodes/sensors.<sup>125</sup> A low-cost plastic-based microfluidic arsenic sensor comprised of an ink-based three-electrode system used for rapid and point-of-use water quality monitoring. A water sample is applied to the sensing system and hand-held analyzer runs a voltammetric test on the sample to determine arsenic concentration.<sup>126</sup>

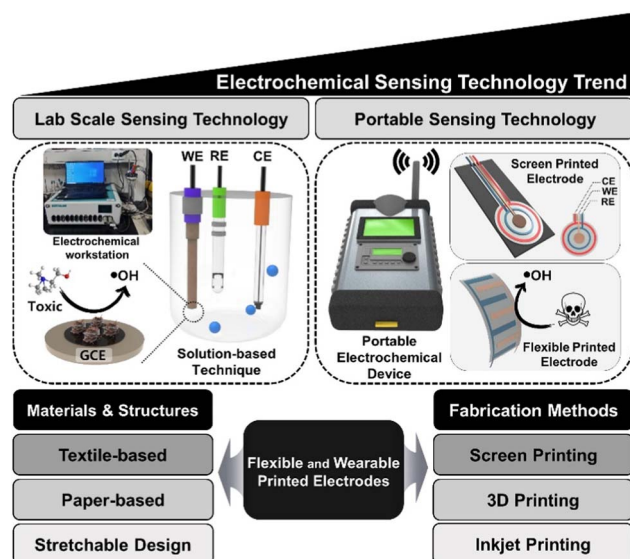


Fig. 15 Schematic overview comparing laboratory-scale based electrochemical device *vs.* portable electrochemical device, classical electrodes *vs.* screen-printed electrodes, and fabrication methods of printed electrodes<sup>125</sup> (reprinted from ref. 125; Copyright (2022), with permission from Elsevier).



**2.5.2. Electroanalytical techniques in arsenic detection & determination.** All electrochemical methods & electroanalytical techniques aim for LODs below the WHO guideline value of 10 ppb. Despite numerous publications in this field during the last decade with respect to novel electrode materials and electrolytes, reproducibility of electrochemical detection is still problematic and the analysis of arsenic in real ground-water samples is far from certain or trivial. Considerable efforts are still needed to develop electrode materials and analytical procedures for

a reliable detection and determination of arsenic with sub-ppb levels in the presence of endogenous toxic metals and organics in water matrices.<sup>16</sup> Different nanoparticles and nanomaterials have been employed for electrode modification and to enhance the efficiency and improve detection limits. Table 7 lists different electrode and modifier materials, electroanalytical techniques and LOD values from the review of recent arsenic research publications. Electrochemical techniques and methods have an inherent advantage with regards to

**Table 7** List of electrode materials and electro-analytical techniques summarising the arsenic detection limits

Electrode modifier <sup>a</sup>	Electrode <sup>a</sup>	Electrochemical technique <sup>b</sup>	LOD (ppb)	References
Au(NPs)	GCE	SWASV	0.025	132
Au(NPs)	Boron-doped diamond	DPASV	0.005	133
Au(NPs)	GCE	SWASV	0.28	134
Au(NPs)	Ultra-micro electrode	SWASV	0.05	135
Au(NPs)	Nanoelectrode ensemble	SWASV	0.005	136
Au(NPs)	GCE	LSV, SWV	0.0096	137
Au(NPs)	GCE	ASV	0.25	138
Au(NPs)	GCE	SWASV	0.15	139
Au(NPs)/MWCNT	GCE	LSV, SWASV	0.1	140
Pt(NPs)	GCE	CV, LSV	2.1	141
Ru(NPs)	GCE	DPV	0.1	142
Au–Cu bimetallic	GCE	SWASV	2.09	143
Au–Pd bimetallic	GCE	ASV	0.25	144
Au NP layer from Au/Si alloy	SPE	CV, DPASV	0.22	145
Au(NPs)	GCE	DPV, CV, ASV, LSV	0.9	146
Au–Pt bimetallic	GCE	LSASV	0.28	147
<b>Oxides</b>				
MnOx/Au NP	GCE	LSASV	0.057	148
Mesoporous MnFe <sub>2</sub> O <sub>4</sub>	GCE	SWASV	3.37	149
Fe <sub>3</sub> O <sub>4</sub> /ionic liquids	GCE	SWASV	0.0008	150
SnO <sub>2</sub> NP	Graphite pencil electrode	CV	10	151
Fe <sub>3</sub> O <sub>4</sub> /reduced graphene oxide nanocomposite	GCE	SWASV	0.38	152
CoO	GCE	CV, amperometry	0.825	153
Au NP/polyaniline	GCE	CV, ASV	0.4	154
Pt nanotube array	GCE	LSV	0.1	155
AuNPs/CeO <sub>2</sub> –ZrO <sub>2</sub>	GCE	CV, CA, SWASV	0.137	156
IrO <sub>x</sub>	Boron-doped diamond	CV	0.15	157
Bismuth film electrode	Bismuth film electrode is formed <i>in situ</i> with arsenic	DPASV	0.012	158
Silane grafted bentonite modified CPE	CPE	ASV	0.0036	159
Graphene/PbO <sub>2</sub>	GCE	SWASV	0.01	160
Pt–Fe(III)/MWCNT	GCE	ASV	0.75	161
Graphene oxide–Au NP	GCE	LSV	0.2	162
CNT–Au NP	SPE	LSV	0.5	163
Carbon black–Au NP nanocomposite	SPE	LSV	0.4	164
<b>Other type of electrodes</b>				
Nafion–AuNP composite	GCE	SWASV	0.047	165
AuNP	SPE	CV, DPASV	0.11	166
Au film	Plastic electrode	DPSV	5	167
AuNP	Carbon microfibre electrode	CV, DPV	0.9	168
Carbon nanotube/Au (NPs)	Carbon nanotube flow-through membrane electrode membrane	ASV	0.75	169
DWCNT/graphene/cholesterol oxidase	SPE	CV, SWV	0.287	128

<sup>a</sup> Au(NPs)/AuNP: gold nanoparticles. Ru(NPs): ruthenium nanoparticles. MWCNT: multi-walled carbon nanotubes. GCE: glassy carbon electrode. CPE: carbon-paste electrode. SPE: screen-printed electrode. BDD: boron-doped diamond. UME: ultramicroelectrode. <sup>b</sup> CV: cyclic voltammetry. ASV: anodic stripping voltammetry. CA: chronoamperometry. DPV: differential pulse voltammetry. SWV: square wave voltammetry. SWASV: square wave anodic stripping voltammetry. DPASV: differential pulse anodic stripping voltammetry. LSASV: linear sweep anodic stripping voltammetry. DPSV: differential pulse stripping voltammetry.



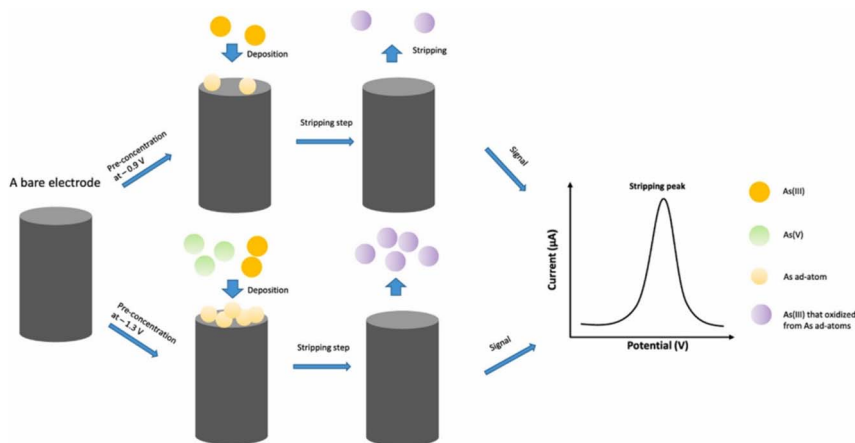


Fig. 16 The total arsenic concentration measured by deposition at  $-1.3$  V while the  $\text{As(III)}$  measured at  $-0.9$  V on gold macroelectrodes based on the underpotential deposition (UPD) of As ad-atoms<sup>131</sup> (reprinted from ref. 131; Copyright (2022), with permission from Elsevier).

miniaturisation and possibly higher sensitivity and lower detection limits.<sup>127</sup>

Thakkar *et al.* made a detailed review of arsenic detection methodologies with LODs of  $<10$  ppb (WHO guideline value). They have critically compared the methods in terms of their potential to detect different arsenic species *e.g.*  $\text{As(III)}$  and  $\text{As(V)}$  in drinking water in the presence of interference from other ions.<sup>17</sup> According to Duoc and colleagues, a novel electrochemical sensor containing double-walled carbon nanotubes (DWCNTs) and a graphene hybrid thin film was discussed for  $\text{As(V)}$  detection.<sup>128</sup> The hybrid thin films based on DWCNTs and graphene have been prepared for electrochemical sensing applications. The hybrid films were synthesised on polycrystalline copper foil by thermal chemical vapor deposition under low pressure. This carbonaceous hybrid film has exhibited high transparency with a transmittance of 94.3%. The occurrence of this hybrid material on the electrode surface of screen-printed electrodes was found to increase electroactive surface area by 1.4 times, whereas electrochemical current was enhanced by 2.4 times. This highly transparent and conductive hybrid film was utilised as a transducing platform of an enzymatic electrochemical  $\text{As(V)}$  biosensor and showed the linear range from 1–10 ppb, with an LOD as low as 0.287 ppb.<sup>128</sup>

AuNPs–polyaniline nanosheet array on iron containing carbon nanofiber (Au–PANI–Fe–CNFs composite) was reported as sensing platform for the determination of  $\text{As(III)}$ .<sup>129</sup> The Au–PANI–Fe–CNFs composite was constructed by the formation of polyaniline (PANI) nanosheet array on the electrospun Fe-containing carbon nanofibers (Fe–CNFs) substrate and self-deposition of Au nanoparticles. PANI presents a uniform array structure on the fiber surfaces and Au nanoparticles ( $20 \pm 6$  nm) were deposited uniformly on the PANI nanosheet surface by means of the reducing property of PANI. The presence and role of Fe in the CNFs was mentioned to accelerate the growth of PANI nanosheet and improves the arsenic adsorption in the sensing process of  $\text{As(III)}$ . The Au–PANI–Fe–CNFs sensor exhibit excellent electrochemical performance for the detection of  $\text{As(III)}$  in water (linear range 5–400 ppb with an LOD of 0.5 ppb,

$S/N \geq 3$ ) and attributed to the unique structure of PANI array and uniform AuNPs distribution.<sup>129</sup> According to Bu *et al.*, a new material of 3D porous graphitic carbon nitride ( $\text{g-C}_3\text{N}_4$ ) decorated by gold nanoparticles (AuNPs/ $\text{g-C}_3\text{N}_4$ ) was designed using a mesoporous molecular sieve (SBA-15) as the sacrificial template.<sup>130</sup> The reported AuNPs/ $\text{g-C}_3\text{N}_4$ /GCE electrode demonstrates superiorities compared to AuNPs/GCE prepared by electrochemical deposition, highlighting the specialties of  $\text{g-C}_3\text{N}_4$  in increasing activity and sensitivity with an extremely low LOD of 0.22 ppb.<sup>130</sup> Zhang and Compton recently reported the use of anodic stripping voltammetry (ASV) allowing sub 10 ppb measurement of total As and  $\text{As(III)}$  in water using the gold macroelectrodes and based on the underpotential deposition (UPD) of As ad-atoms (Fig. 16).<sup>131</sup> The detection of  $\text{As(III)}$  or total arsenic can be selectively made by changing deposition potential (total As content by deposition at  $-1.3$  V and  $\text{As(III)}$  at  $-0.9$  V, linear responses were observed in the range 0.01–0.1  $\mu\text{M}$ ). The analytical signals were recorded at concentrations as low as 0.01  $\mu\text{M}$  (0.8 ppb) for both arsenic species which suggests that this method could be used to detect total arsenic concentrations in drinking water within the WHO threshold value of 10 ppb. The  $\text{As(V)}$  concentration can be determined by subtraction from the total arsenic concentration of the  $\text{As(III)}$  concentration.

### 3. Conclusion

Water is an essential resource for the sustainability of human life and contributes to the economic development and healthy performance of our world ecosystems. Groundwater provides an important drinking water source to many millions of populations across the globe, but it also poses the greatest threat and detrimental effects on the human health if polluted with the toxicants such as arsenic. The impact of arsenic contaminated water on human health is of serious concern and the methods aimed only to reduce the arsenic content to  $\leq 10$  ppb are not a complete solution as the health hazards of arsenic ingestion are dependent on the total accumulated arsenic in the body.







- extract of fresh cod liver by RP-HPLC with simultaneous ICP-MS and ESI-Q-TOF-MS detection, *Food Chem.*, 2013, **141**, 3093–3102.
- 47 S. A. Viczek, K. B. Jensen and K. A. Francesconi, Arsenic-Containing Phosphatidylcholines: A New Group of Arsenolipids Discovered in Herring Caviar, *Angew. Chem.*, 2016, **128**, 5345–5348.
- 48 D. Xie, J. Mattusch and R. Wennrich, Separation of Organoarsenicals by Means of Zwitterionic Hydrophilic Interaction Chromatography (ZIC®-HILIC) and Parallel ICP-MS/ESI-MS Detection, *Eng. Life Sci.*, 2008, **8**, 582–588.
- 49 L. M. Frensemeier, L. Büter, M. Vogel and U. Karst, Investigation of the oxidative transformation of roxarsone by electrochemistry coupled to hydrophilic interaction liquid chromatography/mass spectrometry, *J. Anal. At. Spectrom.*, 2017, **32**, 153–161.
- 50 W. Y. Lee, Y.-H. Yim, E. Hwang, Y. Lim, T. K. Kim and K.-S. Lee, Development of isotope dilution LC-MS/MS method for accurate determination of arsenobetaine in oyster certified reference material, *Bull. Korean Chem. Soc.*, 2014, **35**, 821–827.
- 51 M. Á. García-Sevillano, T. García-Barrera, F. Navarro-Roldán, Z. Montero-Lobato and J. L. Gómez-Ariza, A combination of metallomics and metabolomics studies to evaluate the effects of metal interactions in mammals. Application to *Mus musculus* mice under arsenic/cadmium exposure, *J. Proteomics*, 2014, **104**, 66–79.
- 52 B. Chen, X. Lu, S. Shen, L. L. Arnold, S. M. Cohen and X. C. Le, Arsenic Speciation in the Blood of Arsenite-Treated F344 Rats, *Chem. Res. Toxicol.*, 2013, **26**, 952–962.
- 53 A. C. Schmidt, B. Fahlbusch and M. Otto, Size exclusion chromatography coupled to electrospray ionization mass spectrometry for analysis and quantitative characterization of arsenic interactions with peptides and proteins, *J. Mass Spectrom.*, 2009, **44**, 898–910.
- 54 Z. Yang, H. Peng, X. Lu, Q. Liu, R. Huang, B. Hu, G. Kachanoski, M. J. Zuidhof and X. C. Le, Arsenic Metabolites, Including N-Acetyl-4-hydroxy-m-arsanilic Acid, *Environ. Sci. Technol.*, 2016, **50**, 6737–6743.
- 55 B. Daus, J. Mattusch, R. Wennrich and H. Weiss, Analytical investigations of phenyl arsenicals in groundwater, *Talanta*, 2008, **75**, 376–379.
- 56 Ş. Özcan, S. Bakirdere and O. Y. Ataman, Speciation of arsenic in fish by high-performance liquid chromatography-inductively coupled plasma-mass spectrometry, *Anal. Lett.*, 2016, **49**, 2501–2512.
- 57 J. Gao, H. Yang and B. Li, Investigating the Roles of Dissolved Organic Matter on Arsenic Mobilization and Speciation in Environmental Water, *Clean: Soil, Air, Water*, 2016, **44**, 818–828.
- 58 M. Ponthieu, P. Pinel-Raffaitin, I. Le Hecho, L. Mazeas, D. Amouroux, O. F. Donard and M. Potin-Gautier, Speciation analysis of arsenic in landfill leachate, *Water Res.*, 2007, **41**, 3177–3185.
- 59 Q. Liu, X. Lu, H. Peng, A. Popowich, J. Tao, J. S. Uppal, X. Yan, D. Boe and X. C. Le, Speciation of arsenic – A review of phenylarsenicals and related arsenic metabolites, *TrAC, Trends Anal. Chem.*, 2018, **104**, 171–182.
- 60 V. A. T. Reis and A. C. Duarte, Analytical methodologies for arsenic speciation in macroalgae: A critical review, *TrAC, Trends Anal. Chem.*, 2018, **102**, 170–184.
- 61 Q. Liu, H. Peng, X. Lu and X. C. Le, Enzyme-assisted extraction and liquid chromatography mass spectrometry for the determination of arsenic species in chicken meat, *Anal. Chim. Acta*, 2015, **888**, 1–9.
- 62 H. Peng, B. Hu, Q. Liu, J. Li, X.-F. Li, H. Zhang and X. C. Le, Methylated Phenylarsenical Metabolites Discovered in Chicken Liver, *Angew. Chem., Int. Ed.*, 2017, **56**, 6773–6777.
- 63 S. Braeuer, J. Borovička, T. Glasnov, G. Guedes de la Cruz, K. B. Jensen and W. Goessler, Homoarsenocholine – A novel arsenic compound detected for the first time in nature, *Talanta*, 2018, **188**, 107–110.
- 64 A. Raab, C. Newcombe, D. Pitton, R. Ebel and J. Feldmann, Comprehensive Analysis of Lipophilic Arsenic Species in a Brown Alga (*Saccharina latissima*), *Anal. Chem.*, 2013, **85**, 2817–2824.
- 65 T. Narukawa, E. Matsumoto, T. Nishimura and A. Hioki, Reversed Phase Column HPLC-ICP-MS Conditions for Arsenic Speciation Analysis of Rice Flour, *Anal. Sci.*, 2015, **31**, 521–527.
- 66 H. Cheng, W. Zhang, Y. Wang and J. Liu, Graphene oxide as a stationary phase for speciation of inorganic and organic species of mercury, arsenic and selenium using HPLC with ICP-MS detection, *Microchim. Acta*, 2018, **185**, 425.
- 67 X. Gong, G. Liu, Y. Li, D. Y. W. Yu and W. Y. Teoh, Functionalized-Graphene Composites: Fabrication and Applications in Sustainable Energy and Environment, *Chem. Mater.*, 2016, **28**, 8082–8118.
- 68 A. Suda, K. Baba, I. Akahane and T. Makino, Use of water-treatment residue containing polysilicate-iron to stabilize arsenic in flooded soils and attenuate arsenic uptake by rice (*Oryza sativa* L.) plants, *Soil Sci. Plant Nutr.*, 2016, **62**, 111–116.
- 69 D. G. Kinniburgh and W. Kosmus, Arsenic contamination in groundwater: some analytical considerations, *Talanta*, 2002, **58**, 165–180.
- 70 M. M. Rahman, D. Mukherjee, M. K. Sengupta, U. K. Chowdhury, D. Lodh, C. R. Chanda, S. Roy, M. Selim, Q. Quamruzzaman, A. H. Milton, S. M. Shahidullah, M. T. Rahman and D. Chakraborti, Effectiveness and Reliability of Arsenic Field Testing Kits: Are the Million Dollar Screening Projects Effective or Not?, *Environ. Sci. Technol.*, 2002, **36**, 5385–5394.
- 71 M. Arora, M. Megharaj and R. Naidu, Arsenic testing field kits: some considerations and recommendations, *Environ. Geochem. Health*, 2009, **31**, 45–48.
- 72 S. P. Pande, L. S. Deshpande and S. Kaul, Laboratory and field assessment of arsenic testing field kits in Bangladesh and West Bengal, India, *Environ. Monit. Assess.*, 2001, **68**, 1–18.
- 73 C. M. Steinmaus, C. M. George, D. A. Kalman and A. H. Smith, Evaluation of two new arsenic field test kits



- capable of detecting arsenic water concentrations close to 10 µg/L, *Environ. Sci. Technol.*, 2006, **40**, 3362–3366.
- 74 A. Safarzadeh-Amiri, P. Fowlie, A. Kazi, S. Siraj, S. Ahmed and A. Akbor, Validation of analysis of arsenic in water samples using Wagtech Digital Arsenator, *Sci. Total Environ.*, 2011, **409**, 2662–2667.
- 75 T. Okazaki, H. Kuramitsu, N. Hata, S. Taguchi, K. Murai and K. Okauchi, Visual colorimetry for determination of trace arsenic in groundwater based on improved molybdenum blue spectrophotometry, *Anal. Methods*, 2015, **7**, 2794–2799.
- 76 Y. He, J. Liu, Y. Duan, X. Yuan, L. Ma, R. Dhar and Y. Zheng, A critical review of on-site inorganic arsenic screening methods, *J. Environ. Sci.*, 2022, **125**, 453–469.
- 77 S. K. Ghosh, S. Kundu, M. Mandal and T. Pal, Silver and gold nanocluster catalyzed reduction of methylene blue by arsine in a micellar medium, *Langmuir*, 2002, **18**, 8756–8760.
- 78 R. R. Reddy, G. D. Rodriguez, T. M. Webster, M. J. Abedin, M. R. Karim, L. Raskin and K. F. Hayes, Evaluation of arsenic field test kits for drinking water: Recommendations for improvement and implications for arsenic affected regions such as Bangladesh, *Water Res.*, 2020, **170**, 115325.
- 79 R. D. Sharma, S. Joshi and S. Amlathe, MATLAB assisted disposable sensors for quantitative determination of arsenic, *Anal. Methods*, 2011, **3**, 452–456.
- 80 P. Nath, R. K. Arun and N. Chanda, A paper based microfluidic device for the detection of arsenic using a gold nanosensor, *RSC Adv.*, 2014, **4**, 59558–59561.
- 81 T. Rupasinghe, T. J. Cardwell, R. W. Cattrall, I. D. Potter and S. D. Kolev, Determination of arsenic by pervaporation-flow injection hydride generation and permanganate spectrophotometric detection, *Anal. Chim. Acta*, 2004, **510**, 225–230.
- 82 S. Kundu, S. K. Ghosh, S. Nath, S. Panigrahi, S. Praharaj, S. Basu and T. Pal, Ion-associate of arsenic (V)-salicylic acid chelate with methylene blue in toluene: application for arsenic quantification, *Indian J. Chem., Sect. A: Inorg., Bio-inorg., Phys., Theor. Anal. Chem.*, 2005, **44**, 2030–2033.
- 83 R. D. Sharma, S. Joshi and S. Amlathe, Quantitative determination and development of sensing devices via a new reagent system for arsenic, *Anal. Chem.*, 2012, **11**, 342–346.
- 84 F. Pena-Pereira, L. Villar-Blanco, I. Lavilla and C. Bendicho, Test for arsenic speciation in waters based on a paper-based analytical device with scanometric detection, *Anal. Chim. Acta*, 2018, **1011**, 1–10.
- 85 D. Paul, S. Dutta and R. Biswas, LSPR enhanced gasoline sensing with a U-bent optical fiber, *J. Phys. D: Appl. Phys.*, 2016, **49**, 305104.
- 86 B. S. Boruah, N. K. Daimari and R. Biswas, Functionalized silver nanoparticles as an effective medium towards trace determination of arsenic (III) in aqueous solution, *Results Phys.*, 2019, **12**, 2061–2065.
- 87 S. Das Chakraborty, S. Mondal, B. Satpati, U. Pal, S. K. De, M. Bhattacharya, S. Ray and D. Senapati, Wide Range Morphological Transition of Silver Nanoprisms by Selective Interaction with As (III): Tuning–Detuning of Surface Plasmon Offers To Decode the Mechanism, *J. Phys. Chem. C*, 2019, **123**, 11044–11054.
- 88 S.-Y. Chen, W. Wei, B.-C. Yin, Y. Tong, J. Lu and B.-C. Ye, Development of a highly sensitive whole-cell biosensor for arsenite detection through engineered promoter modifications, *ACS Synth. Biol.*, 2019, **8**, 2295–2302.
- 89 K. Siegfried, C. Endes, A. F. M. K. Bhuiyan, A. Kuppardt, J. r. Mattusch, J. R. van der Meer, A. Chatzinotas and H. Harms, Field testing of arsenic in groundwater samples of Bangladesh using a test kit based on lyophilized bioreporter bacteria, *Environ. Sci. Technol.*, 2012, **46**, 3281–3287.
- 90 A. J. Meyer, T. H. Segall-Shapiro, E. Glassey, J. Zhang and C. A. Voigt, Escherichia coli “Marionette” strains with 12 highly optimized small-molecule sensors, *Nat. Chem. Biol.*, 2019, **15**, 196–204.
- 91 F. Zhang, J. M. Carothers and J. D. Keasling, Design of a dynamic sensor-regulator system for production of chemicals and fuels derived from fatty acids, *Nat. Biotechnol.*, 2012, **30**, 354–359.
- 92 D. Clark, N. Pazdernik and M. McGehee, Chapter 16–regulation of transcription in Prokaryotes, *Mol. Biol.*, 2019, 522–559.
- 93 A. Carlin, W. Shi, S. Dey and B. P. Rosen, The ars operon of Escherichia coli confers arsenical and antimonial resistance, *J. Bacteriol.*, 1995, **177**, 981–986.
- 94 B. P. Rosen, Resistance mechanisms to arsenicals and antimonials, *J. Basic Clin. Physiol. Pharmacol.*, 1995, **6**, 251–264.
- 95 E. Diesel, M. Schreiber and J. R. van der Meer, Development of bacteria-based bioassays for arsenic detection in natural waters, *Anal. Bioanal. Chem.*, 2009, **394**, 687–693.
- 96 H. Kaur, R. Kumar, J. N. Babu and S. Mittal, Advances in arsenic biosensor development—a comprehensive review, *Biosens. Bioelectron.*, 2015, **63**, 533–545.
- 97 X. Wang, K. Zhu, D. Chen, J. Wang, X. Wang, A. Xu, L. Wu, L. Li and S. Chen, Monitoring arsenic using genetically encoded biosensors *in vitro*: The role of evolved regulatory genes, *Ecotoxicol. Environ. Saf.*, 2021, **207**, 111273.
- 98 X. Jia, R. Bu, T. Zhao and K. Wu, Sensitive and specific whole-cell biosensor for arsenic detection, *Appl. Environ. Microbiol.*, 2019, **85**, 006944, DOI: [10.1128/AEM.00694-19](https://doi.org/10.1128/AEM.00694-19).
- 99 S. Sánchez, M. McDonald, D. M. Silver, S. de Bonnault, C. Chen, K. LeBlanc, E. C. Hicks and R. M. Mayall, The Integration of Whole-Cell Biosensors for the Field-Ready Electrochemical Detection of Arsenic, *J. Electrochem. Soc.*, 2021, **168**, 067508.
- 100 K. Mao, H. Zhang, Z. Wang, H. Cao, K. Zhang, X. Li and Z. Yang, Nanomaterial-based aptamer sensors for arsenic detection, *Biosens. Bioelectron.*, 2020, **148**, 111785.
- 101 B. Liu and J. Liu, DNA adsorption by magnetic iron oxide nanoparticles and its application for arsenate detection, *Chem. Commun.*, 2014, **50**, 8568–8570.
- 102 M. Oroval, C. Coll, A. Bernardos, M. D. Marcos, R. Martinez-Manez, D. G. Shchukin and F. Sancenon, Selective fluorogenic sensing of As (III) using aptamer-capped



- nanomaterials, *ACS Appl. Mater. Interfaces*, 2017, **9**, 11332–11336.
- 103 A. A. Ensafi, N. Kazemifard and B. Rezaei, A simple and sensitive fluorimetric aptasensor for the ultrasensitive detection of arsenic (III) based on cysteamine stabilized CdTe/ZnS quantum dots aggregation, *Biosens. Bioelectron.*, 2016, **77**, 499–504.
- 104 L. Zhang, X.-Z. Cheng, L. Kuang, A.-Z. Xu, R.-P. Liang and J.-D. Qiu, Simple and highly selective detection of arsenite based on the assembly-induced fluorescence enhancement of DNA quantum dots, *Biosens. Bioelectron.*, 2017, **94**, 701–706.
- 105 Y. Wu, S. Zhan, F. Wang, L. He, W. Zhi and P. Zhou, Cationic polymers and aptamers mediated aggregation of gold nanoparticles for the colorimetric detection of arsenic (III) in aqueous solution, *Chem. Commun.*, 2012, **48**, 4459–4461.
- 106 Y. Wu, L. Liu, S. Zhan, F. Wang and P. Zhou, Ultrasensitive aptamer biosensor for arsenic (III) detection in aqueous solution based on surfactant-induced aggregation of gold nanoparticles, *Analyst*, 2012, **137**, 4171–4178.
- 107 S. Zhan, M. Yu, J. Lv, L. Wang and P. Zhou, Colorimetric detection of trace arsenic (III) in aqueous solution using arsenic aptamer and gold nanoparticles, *Aust. J. Chem.*, 2014, **67**, 813–818.
- 108 Y. Wu, F. Wang, S. Zhan, L. Liu, Y. Luo and P. Zhou, Regulation of hemin peroxidase catalytic activity by arsenic-binding aptamers for the colorimetric detection of arsenic (III), *RSC Adv.*, 2013, **3**, 25614–25619.
- 109 F. Divsar, K. Habibzadeh, S. Shariati and M. Shahriarinnour, Aptamer conjugated silver nanoparticles for the colorimetric detection of arsenic ions using response surface methodology, *Anal. Methods*, 2015, **7**, 4568–4576.
- 110 L. Zeng, D. Zhou, J. Gong, C. Liu and J. Chen, Highly sensitive aptasensor for trace arsenic (III) detection using DNAzyme as the biocatalytic amplifier, *Anal. Chem.*, 2019, **91**, 1724–1727.
- 111 Q.-H. Hou, A.-Z. Ma, D. Lv, Z.-H. Bai, X.-L. Zhuang and G.-Q. Zhuang, The impacts of different long-term fertilization regimes on the bioavailability of arsenic in soil: integrating chemical approach with *Escherichia coli* arsRp:: luc-based biosensor, *Appl. Microbiol. Biotechnol.*, 2014, **98**, 6137–6146.
- 112 P. Sharma, S. Asad and A. Ali, Bioluminescent bioreporter for assessment of arsenic contamination in water samples of India, *J. Biosci.*, 2013, **38**, 251–258.
- 113 F. Cortés-Salazar, S. Beggah, J. R. van der Meer and H. H. Girault, Electrochemical As (III) whole-cell based biochip sensor, *Biosens. Bioelectron.*, 2013, **47**, 237–242.
- 114 M. S. R. Siddiki, S. Shimoaoki, S. Ueda and I. Maeda, Thermoresponsive magnetic nano-biosensors for rapid measurements of inorganic arsenic and cadmium, *Sensors*, 2012, **12**, 14041–14052.
- 115 K. Yoshida, K. Inoue, Y. Takahashi, S. Ueda, K. Isoda, K. Yagi and I. Maeda, Novel carotenoid-based biosensor for simple visual detection of arsenite: characterization and preliminary evaluation for environmental application, *Appl. Environ. Microbiol.*, 2008, **74**, 6730–6738.
- 116 K. Matsunaga, Y. Okuyama, R. Hirano, S. Okabe, M. Takahashi and H. Satoh, Development of a simple analytical method to determine arsenite using a DNA aptamer and gold nanoparticles, *Chemosphere*, 2019, **224**, 538–543.
- 117 D. Zhang, Y. Liu, J. Ding, K. Hayat, X. Zhan, P. Zhou and D. Zhang, Label-free colorimetric assay for arsenic (III) determination based on a truncated short ssDNA and gold nanoparticles, *Microchim. Acta*, 2021, **188**, 1–9.
- 118 A. Bakhrat, E. Eltzov, Y. Finkelstein, R. S. Marks and D. Raveh, UV and arsenate toxicity: a specific and sensitive yeast bioluminescence assay, *Cell Biol. Toxicol.*, 2011, **27**, 227–236.
- 119 S.-I. Choe, F. N. Gravelat, Q. Al Abdallah, M. J. Lee, B. F. Gibbs and D. C. Sheppard, Role of *Aspergillus niger* *acrA* in arsenic resistance and its use as the basis for an arsenic biosensor, *Appl. Environ. Microbiol.*, 2012, **78**, 3855–3863.
- 120 F. Truffer, N. Buffi, D. Merulla, S. Beggah, H. Van Lintel, P. Renaud, J. R. van der Meer and M. Geiser, Compact portable biosensor for arsenic detection in aqueous samples with *Escherichia coli* bioreporter cells, *Rev. Sci. Instrum.*, 2014, **85**, 015120.
- 121 Y. Liu and W. Wei, Layer-by-layer assembled DNA functionalized single-walled carbon nanotube hybrids for arsenic (III) detection, *Electrochem. Commun.*, 2008, **10**, 872–875.
- 122 P. R. Solanki, N. Prabhakar, M. K. Pandey and B. D. Malhotra, Surface plasmon resonance-based DNA biosensor for arsenic trioxide detection, *J. Environ. Anal. Chem.*, 2009, **89**, 49–57.
- 123 Q. Zhou, L. Zhang and H. Wu, Nanomaterials for cancer therapies, *Nanotechnol. Rev.*, 2017, **6**, 473–496.
- 124 C. Zhu, G. Yang, H. Li, D. Du and Y. Lin, Electrochemical sensors and biosensors based on nanomaterials and nanostructures, *Anal. Chem.*, 2015, **87**, 230–249.
- 125 R. Umaphathi, S. M. Ghoreishian, S. Sonwal, G. M. Rani and Y. S. Huh, Portable electrochemical sensing methodologies for on-site detection of pesticide residues in fruits and vegetables, *Coord. Chem. Rev.*, 2022, **453**, 214305.
- 126 U. Kim, J. VanderGiessen, B. Demaree, M. Reynolds and K. Perricone, Development of low-cost plastic microfluidic sensors toward rapid and point-of-use detection of arsenic in drinking water for global health, *IEEE Trans. Biomed. Circuits Syst.*, 2013, 113–117.
- 127 T. O. Hara and B. Singh, Electrochemical biosensors for detection of pesticides and heavy metal toxicants in water: recent trends and progress, *ACS ES&T Water*, 2021, **1**, 462–478.
- 128 P. N. D. Duoc, N. H. Binh, T. Van Hau, C. T. Thanh, P. Van Trinh, N. V. Tuyen, N. Van Quynh, N. Van Tu, V. D. Chinh and V. T. Thu, A novel electrochemical sensor based on double-walled carbon nanotubes and graphene hybrid thin film for arsenic (V) detection, *J. Hazard. Mater.*, 2020, **400**, 123185.





- 156 M. Yang, P.-H. Li, W.-H. Xu, Y. Wei, L.-N. Li, Y.-Y. Huang, Y.-F. Sun, X. Chen, J.-H. Liu and X.-J. Huang, Reliable electrochemical sensing arsenic(III) in nearly groundwater pH based on efficient adsorption and excellent electrocatalytic ability of AuNPs/CeO<sub>2</sub>-ZrO<sub>2</sub> nanocomposite, *Sens. Actuators, B*, 2018, **255**, 226–234.
- 157 A. Salimi, M. E. Hyde, C. E. Banks and R. G. Compton, Boron doped diamond electrode modified with iridium oxide for amperometric detection of ultra trace amounts of arsenic(iii), *Analyst*, 2004, **129**, 9–14.
- 158 J. Long and Y. Nagaosa, Determination of trace arsenic(III) by differential-pulse anodic stripping voltammetry with *in situ* plated bismuth-film electrode, *Int. J. Environ. Anal. Chem.*, 2008, **88**, 51–60.
- 159 J. Lalmalsawmi, Z. Zirlianngura, D. Tiwari and S. M. Lee, Low cost, highly sensitive and selective electrochemical detection of arsenic (III) using silane grafted based nanocomposite, *Environ. Eng. Res.*, 2020, **25**, 579–587.
- 160 G. K. Ramesha and S. Sampath, *In situ* formation of graphene-lead oxide composite and its use in trace arsenic detection, *Sens. Actuators, B*, 2011, **160**, 306–311.
- 161 S.-H. Shin and H.-G. Hong, Anodic Stripping Voltammetric Detection of Arsenic (III) at Platinum-Iron (III) Nanoparticle Modified Carbon Nanotube on Glassy Carbon Electrode, *Bull. Korean Chem. Soc.*, 2010, **31**, 3077–3083.
- 162 Y. Liu, Z. Huang, Q. Xie, L. Sun, T. Gu, Z. Li, L. Bu, S. Yao, X. Tu, X. Luo and S. Luo, Electrodeposition of electroreduced graphene oxide-Au nanoparticles composite film at glassy carbon electrode for anodic stripping voltammetric analysis of trace arsenic(III), *Sens. Actuators, B*, 2013, **188**, 894–901.
- 163 J. C. M. Gamboa, L. Cornejo and J. A. Squella, Vibrating screen printed electrode of gold nanoparticle-modified carbon nanotubes for the determination of arsenic(III), *J. Appl. Electrochem.*, 2014, **44**, 1255–1260.
- 164 S. Cinti, S. Politi, D. Moscone, G. Palleschi and F. Arduini, Stripping Analysis of As(III) by Means of Screen-Printed Electrodes Modified with Gold Nanoparticles and Carbon Black Nanocomposite, *Electroanalysis*, 2014, **26**, 931–939.
- 165 J.-F. Huang and H.-H. Chen, Gold-nanoparticle-embedded nafion composite modified on glassy carbon electrode for highly selective detection of arsenic(III), *Talanta*, 2013, **116**, 852–859.
- 166 A. P. M. Udayan, B. Kachwala, K. Karthikeyan and S. Gunasekaran, Ultrathin quasi-hexagonal gold nanostructures for sensing arsenic in tap water, *RSC Adv.*, 2020, **10**, 20211–20221.
- 167 W. Wang, N. Bao, W. Yuan, N. Si, H. Bai, H. Li and Q. Zhang, Simultaneous determination of lead, arsenic, and mercury in cosmetics using a plastic based disposable electrochemical sensor, *Microchem. J.*, 2019, **148**, 240–247.
- 168 P. Carrera, P. J. Espinoza-Montero, L. Fernández, H. Romero and J. Alvarado, Electrochemical determination of arsenic in natural waters using carbon fiber ultra-microelectrodes modified with gold nanoparticles, *Talanta*, 2017, **166**, 198–206.
- 169 A. Buffa and D. Mandler, Arsenic(III) detection in water by flow-through carbon nanotube membrane decorated by gold nanoparticles, *Electrochim. Acta*, 2019, **318**, 496–503.

